UNITED NATIONS UNIVERSITY
GEOTHERMAL TRAINING PROGRAMME
Orkustofnun, Grensásvegur 9,
IS-108 Reykjavík, Iceland

Reports 2011
Number 18

INTERPRETATION OF GEOCHEMICAL WELL TEST DATA FOR WELL NWS-6D, NW-SABALAN, IRAN: AN IMPLICATION FOR SCALING POTENTIAL AND RECOMMENDED INHIBITION METHODS

Abdullah Kosari Torbehbar
SUNA – Renewable Energy Organization of Iran
Yadegare Imam Highway, Poonake Bakhtari Ave., Shahrake Ghods
P.O. Box 14155-6398, Tehran
IRAN
abdullahkosari@gmail.com

ABSTRACT

Well NWS-6D is the sixth drilled well in the second stage of exploration and development in Northwest Sabalan Geothermal field, NW Iran, and the third to be discharged. Based on previous investigations on alteration mineralogy and the measured temperature of the well, a temperature of 233°C was selected as the reference temperature for calculating the real chemical composition and temperature of the deep thermal aquifer. The discharged fluids consisted of mature NaCl waters. Fluctuations in some components in the discharged fluids, particularly soon after discharge initiation, could be related to the presence of more than one aquifer in the deep levels. Quartz geothermometers gave an average temperature of 233°C for the deep liquid. When the deep liquid boiled, it became super-saturated with amorphous silica at the average temperature of 122°C. The deep liquid was very close to a calcite saturation state in the quartz temperature range of 229-234°C. Upon boiling the liquid becomes supersaturated with respect to calcite and, as a result, calcite scaling will obviously be the main problem in the production wells. Regarding the prospect of the project in NW Sabalan Geothermal field, a calcite inhibitor system is recommended in the production stage and mechanical cleaning is recommended throughout the long-term discharging of the wells to prevent calcite scaling in the wells.

1. INTRODUCTION

The systematic evaluation of the geothermal resources of Iran was carried out in the 1970s and four main regions of potential geothermal resources including Khoy-Maku, Mount Sabalan, Sahand and Damavand, located on the north and northwest parts of Iran, were identified for more detailed investigation (TB, 1979; ENEL, 1983). The NW-Sabalan (NWS) geothermal prospect, of interest in this report, lies in the Moil valley on the western slopes of Mt. Sabalan, approximately 16 km southeast of Meshkinshahr city (Figure 1). It is recognized as a potential reservoir for power generation purposes.

FIGURE 1: Location of northwest Sabalan geothermal prospect (Noorollahi et al., 1998)

Well NWS-6D is the sixth well of 11 wells drilled in the second stage of exploration and development in NW Sabalan geothermal field. The background studies in NW Sabalan geothermal prospect are presented in detail in Section 2. A chemical evaluation of discharged fluids from well NWS-6 is presented in this study. The study includes an effort to determine the most realistic chemical composition and temperature for the deep aquifer fluid, evaluation of scaling potential in the well, and available and recommended methods for removing the scale from the well.

2. BACKGROUND

2.1 General status of geothermal development

The idea of power generation from NW Sabalan geothermal prospect was initially proposed in 1994; thereafter, this field was made an eminent priority. Since 1998, this region has been a target of detailed exploration, development and drilling. These studies were initially carried out by the Renewable Energy Organization of Iran (SUNA) and Sinclair Knight Merz (SKM) from New Zealand in two stages: the first stage included exploration and a development program during which formerly collected geothermal field data were reviewed. Sampling and analysis of all surface geothermal exposures as well as a detailed MT geophysical survey were also performed, resulting in the determination of five geothermal anomalies in the Mt. Sabalan area. Subsequently, Moil Valley area, the most prospective anomaly, was geologically mapped and a pre-drilling exploration model was formulated. During the second stage, exploration drilling was implemented and three deep exploration and two shallow injection wells were drilled from 2002 to 2004. The wells were tested and, ultimately, NWS1 and NWS4 (Figure 2) turned out to be productive. Numerical modelling of the reservoir was also accomplished from 2004 to 2005 and the capacity of the field was estimated to sustain 55 MW power production (SKM, 2005a). In 2007, a technical team from PNOC Energy Development Corporation (PNOC-EDC), from the Philippines, was assigned to review available data from NW Sabalan, initiate an independent and firm understanding of the hydrological model of the NW Sabalan geothermal field, and furnish SUNA with a more technical basis for its drilling and development program. A new MT survey, re-evaluation of all thermal springs in the area, detailed geological mapping and a new discharge test of wells NWS-1 and NWS-4 were the activities proposed and conducted before drilling in order to determine the centre of the geothermal system.

From 2008 up to time of writing (October 2011), the National Iranian Drilling Company (NIDC) has drilled six more production and injection wells in Sabalan geothermal field and more detailed geophysical and geological investigations were also carried out. Additionally, the characteristics of the Sabalan reservoir are being precisely assessed using well loggings and discharge tests on the production wells. The resulting data will be crucial for future development and/or production steps.

2.2 Geological settings

Mt. Sabalan, site of the NW Sabalan geothermal field, is located in a Quaternary andesitic volcanic complex that covers an area of approximately 2500 km^2 between the Ahar valley in the east, the Qareh Su valley in the west and the Balikhly Chae valley in the south. Tectonically, it lies on the south Caspian plate which underlies the Eurasian plate to the north and overlies the Iranian plate, producing northwestwardly compression (McKenzie, 1972). The area under study is characterized by the predominance of Quaternary terrace deposits (Dizu Formation), altered post-caldera Pliocene trachyandesitic domes, flows and lahars (Kasra Formation), unaltered syn-caldera Pleistocene trachydacite to trachyandesitic flows, domes and lahars (Taos Formation), and pre-caldera trachyandesitic lavas, tuffs and pyroclastics (Valhazir Formation) (SKM, 2005c) (Figure 2). Their age is estimated at 0.9 Ma using the Ar-Ar dating method (Bogie et al., 2000).

Structurally, three main fault systems with NE, NW and N-S trends exist in the area. The last two (NW and N-S) are believed to be conjugate tensional faults between major NE faults. Further cross cutting fault sets include faults with NE to ENE trending north of well NWS-4 and ESE and NNE faults southeast of the well in the Moil Valley (Shadkam Torbati, 2007). Three main arcuate structures have also been identified from satellite images which are interpreted to be the outer caldera, inner caldera and a decollement upon which slippage of the volcanic pile has occurred (Bogie et al., 2000). Faridi et al. (2010) mapped the stucture of the Sabalan volcano and concluded that it is deformed in an active tectonic regime. This deformation has led to the elongation of the Sabalan caldera parallel to the regional σ_3 axis. They concluded that the Sabalan caldera is associated with an extensive hydrothermal system and fracturing in the inner and outer calderas causing the thermal source fluids to readily ascend to the surface.

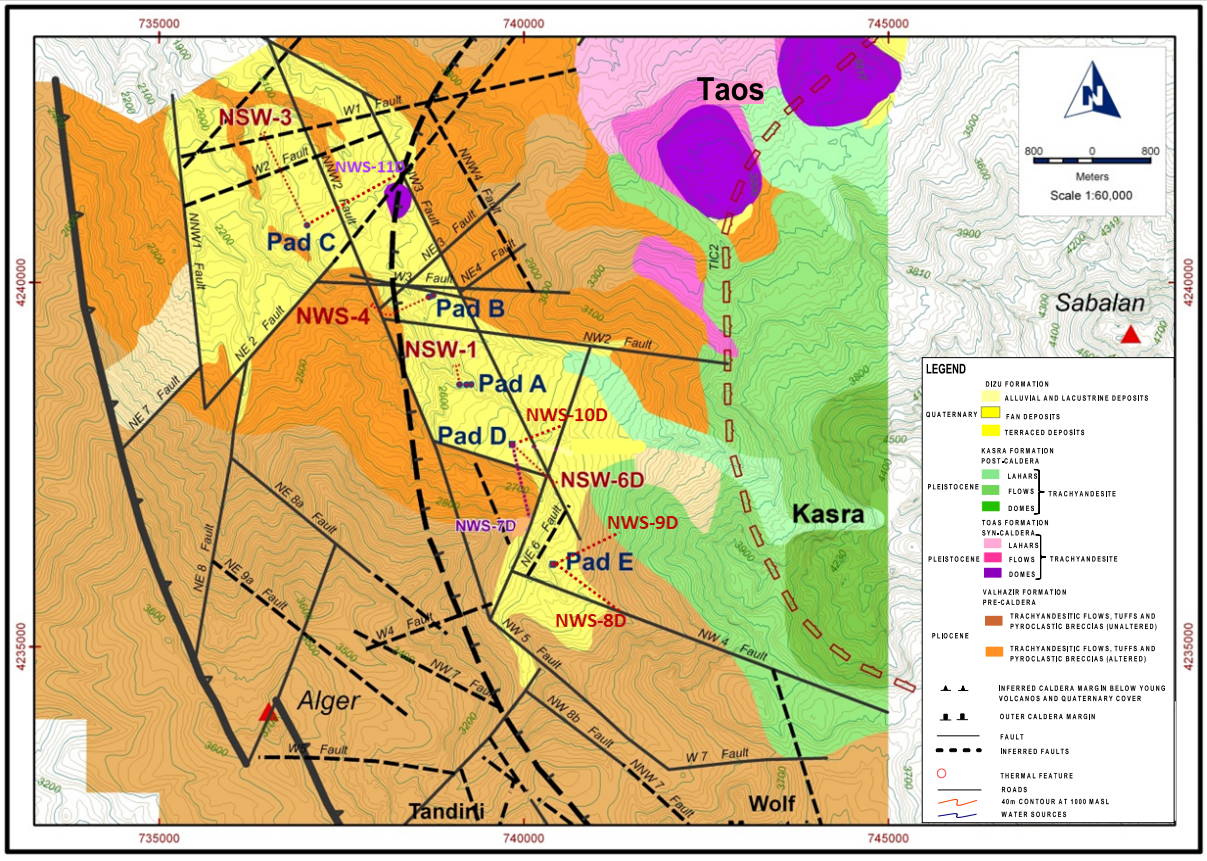

FIGURE 2: Geology of the NW Sabalan geothermal field (modified from Bogie et al., 2000)

3. RESERVOIR CHARACTERISTICS

In order to compute the deep liquid composition of the Sabalan reservoir, using chemical data from discharged fluids, a reference temperature should be established. In this section, the most recent studies of the field are briefly reviewed in order to constrain the reservoir temperature.

3.1 Subsurface geology

Well NWS-6D was the first well drilled in the second stage of exploration. It was targeted to the southeast with an azimuth of ~133°C reaching a total depth of 2500 m MD (2175.7 m VD). As the present geology data on well NWS-6D is constrained to only a core petrographic report, a combination of the other borehole geology data in the area, especially of well NWS-7D which was drilled on the same pad as NWS-6D (Figure 2) but at a different azimuth (~170°C), and of wells NWS-1 and NWS-4, was used to achieve the most reliable concept of the sub-surface lithology and alteration mineralogy. The lithology, hydrothermal mineralogy and estimated temperature of the core samples from wells NWS-6D and NWS-7D and cuttings from well NWS-7D are described by EDC (2009a and 2009b) and briefly presented in Table 1, while the borehole geology of wells NWS-1 and NWS-4 is reported by SKM (2003 and 2004a). The locations of these wells are presented in Figure 2.

The andesite lava and pyroclastic units in NWS-6D (cores 1 and 2) and NWS-7D (core 2) can be correlated with highly altered Tertiary volcanics encountered by earlier wells drilled in NW Sabalan. In NWS-1, these volcanic units were designated as Eocene Volcanics (Epa), while in NWS-4 they were called Early Tertiary volcanics. Core 3 of well NWS-6D is highly altered biotite hornblende micro-monzodiorite porphyry that might be associated with diorite porphyry dikes (Old Diorite Porphyry unit) found in NWS-1 and NWS-4. The dominant assemblage of illitic clays, epidote, quartz, chlorite, anhydrite, and calcite suggests precipitation from hot, neutral-pH fluids. Core 4 of well NWS-7D is an epidote-garnet hornfels. Intense thermal metamorphism has obscured the primary features of the original rock, however a faint relict texture suggests that the parent rock was more likely a tuff breccia. The hornfelsic rock is now composed of clusters of reddish brown melanite to green andradite garnet varieties and epidote in a granoblastic matrix of interlocking quartz, feldspar, and clinopyroxene. Variations in the contact metamorphic fabric along core 4 suggest that only a minor dike or an apophyse of a larger plutonic body (Miocene monzonite) has intruded at this depth, causing partial contact metamorphism of volcanic units (Epa). The two deepest cores of well NWS-7D are both clinopyroxene-garnet-calcite hornfels, likely derived from carbonate sedimentary rocks based on observed texture and mineralogy. They are interpreted to be correlative to Paleozoic Metamorphics earlier identified in well NWS-1 as metamorphosed sandstone. They are composed of granoblastic mosaic of grossular garnet, calcite, clinopyroxene and feldspar. In well NWS-1, a plutonic monzonite body, believed to be Miocene in age, and contact metamorphic biotite hornfels were intersected from 1021 m to 3197 m (TD), but the cored depths in well NWS-7D were unable to intersect the intrusive rocks.

3.2 Alteration mineralogy and estimated temperature

Based on the occurrence of epidote in cores from NWS-6D and NWS-7D, estimated reservoir temperatures in these two wells are comparable with those in NWS-1. At 1500 m depth, the predicted reservoir temperature is ~240°C in NWS-1, as suggested by alteration mineralogy and fluid inclusion data. In NWS-6D, euhedral epidote occurs as a replacement and as vug fills in core 1, indicating temperatures of ~240°C at 1534 m. On the other hand, epidote is also present in core 2 of well NWS-7D, although in anhedral to subhedral form, implying temperatures of ~240-250°C at 1316 m. This predicted temperature is also consistent with those of NWS-1 at comparable levels. Hence, reservoir temperatures at about 1500 m remain almost constant going southeastward from Pad A (NWS-1) to Pad D (NWS-6D, NWS-7D) (Figure 2). Moreover, at deeper reservoir levels,

TABLE 1: Lithology, alteration minerals and predicted temperatures of core samples from wells NWS-6D and NWS-7D (EDC, 2009b) and cutting samples of NWS-7D (2009b)

Well	Core no.	Depth (m MD)	Lithology	Alteration minerals	Possible formation	Estimated temperature (°C)
NWS-6D	Core 1, Part 1	1534.3-1538.7	Andesitic lapilli tuff	Illitic clays, hematite, chlorite, anhydrite	Tertiary volcanics (Valhazir)	~240
	Core 1, Part 3	1534.3-1538.7	Porphyric andesite	Illitic clays, chlorite, incipient-anhedral epidote, quartz, anhydrite, sphenleucoxene, hematite, rare actinolite	Tertiary volcanics (Valhazir)	~240
	Core 1, Part 4	1534.3-1538.7	Andesitic breccia	Illitic clays, anhedral-euhedral epidote, quartz, anhydrite, hematite	Tertiary volcanics (Valhazir)	~240
	Core 2	1834.3-1838.7	Porphyritic trachytic andesite	Anhedral-euhedral epidote, sphene, leucoxene, quartz, calcite, anhydrite, pyrite, illite-smectite, chlorite, rare bornite and sphalerite	Tertiary volcanics (Valhazir)	~240
	Core 3	2070-2071,5	Biotite horn-bland porphyry micro-mon-zonite with synite xenolith	Anhedral-subhedral epidote, illite, chlorite-calcite, anhydrite, sphene	Old diorite porphyry	~240
NWS-7D	Core 2	1316-1319 (1280-1283 m VD)	Andesite porphyric	Incipient epidote, anhedral-subhedral epidote, illite, chlorite, anhydrite, calcite, sphene, leucoxene, hematite	Tertiary volcanics (Valhazir)	~240-250
	Core 4	2179.5-2181 (1981.5-1983 m VD)	Epidot-garnet hornfels	Euhedral to subhedral epidote veins	Partially metamorpho-sed Eocene volcanics (Epa)	≥250
	Core 5	2480-2481.2 (2188-2489.2 m VD)	Clinopyroxene-garnet-calcite hornfels	Illite-smectite, anhedral epidote, laumontite	Paleozoic metamorphics	~220-240
	Core 6	2700-2705 (2260-2265 m VD)	Clinopyroxene-garnet-calcite hornfels	Laumontite	Paleozoic metamorphics	~220-240

temperatures also do not increase significantly, based on alteration mineralogy in NWS-6D. Epidote is still the dominant alteration mineral in the two deeper core samples in NWS-6D, suggesting ~240°C at 1834 m and 2070 m. The absence of higher temperature alteration minerals such as actinolite or

wollastonite indicates a constant temperature for deep thermal fluids. This almost isothermal trend is also observed in NWS-1 where no increase in reservoir temperatures was noted down to 3000 m, based on fluid inclusion studies. Based on the presence of fresh euhedral epidote and clinozoisite veins cutting metamorphosed tuff breccia at ~2180 m depth of NWS-7D (core 4), hot neutral fluids with temperatures of ~250°C are likely flowing. The high-temperature metamorphic assemblage in core 4 has been widely replaced by retrograde hydrothermal minerals of sphene, leucoxene, and minor calcite. From the two deepest cores (cores 5 and 6) of NWS-7D, however, lower fluid temperatures are indicated by a minor amount of low temperature alteration minerals such as lumontite replacing hornfels. This indicates a possible cooling of the reservoir at levels deeper than about 2480 m. It is noticeable that in wells NWS-6D and NWS-7D, calcite and quartz alteration minerals are persistent after 300 m where the wells encountered Tertiary volcanics (Valhazir Formation). Chlorite, smectite and illite-smectite are the other alteration minerals from 300 m to 1000 m depth, where total loss of circulation occurred.

At a few depths between 850 m and 1031 m, alteration minerals were produced by the reaction of rock units with acid fluids. The original rock units had been completely altered into an assemblage of pyrophyllite + diaspore + quartz + pyrite + anhydrite + barite. A rare amount of pale green crystals, suspected to be andalusite, were associated with diaspore and pyrophyllite at 996, 1010 and 1031 m. Pyrophyllite and diaspore are retrograde to low temperature minerals and veins of laumontite + quartz + adularia cut acid altered rocks at 996 m. Hence, these acid minerals are interpreted to be relict alterations, and are not related to the present hydrothermal system in NW Sabalan.

3.3 Temperature and feed zones

Investigations on Sabalan reservoir, using measured temperature and surveyed data, in wells NWS-1, NWS-3, NWS-4, NWS-5D, NWS-6D and NWS-7D by Abdollahzadeh Bina (2009), show that the temperatures of most of the wells are below the boiling point curve, implying that the reservoir does not contain a two-phase mixture of steam and water in the southern part of the area. A temperature cross-section of the area (Figure 3) shows that there is a nearly 700 m thick cap rock, overlying at least a 2 km thick convective zone below approximately 1500 m a.s.l. The hottest upflow of the reservoir that influences NWS-6D's deep temperature flows in a general direction of SE-NW towards well NWS-3. In addition, the temperatures below +1500 m a.s.l (around 1200 m VD) for NWS-5D, NWS-6D and NWS-7D are noticeably close to the boiling point curve. Hence, at an elevation of around +1000 m a.s.l (around 1700 m VD), the highest temperature estimated in NWS-7D is circa 270-280°C. On the basis of this reservoir model, a relatively significant temperature inversion occurs, starting from +1500 m a.s.l and striking at depths between +600 to - 200 m a.s.l (around 2100-2900 m VD) with the temperature range of 230-240°C.

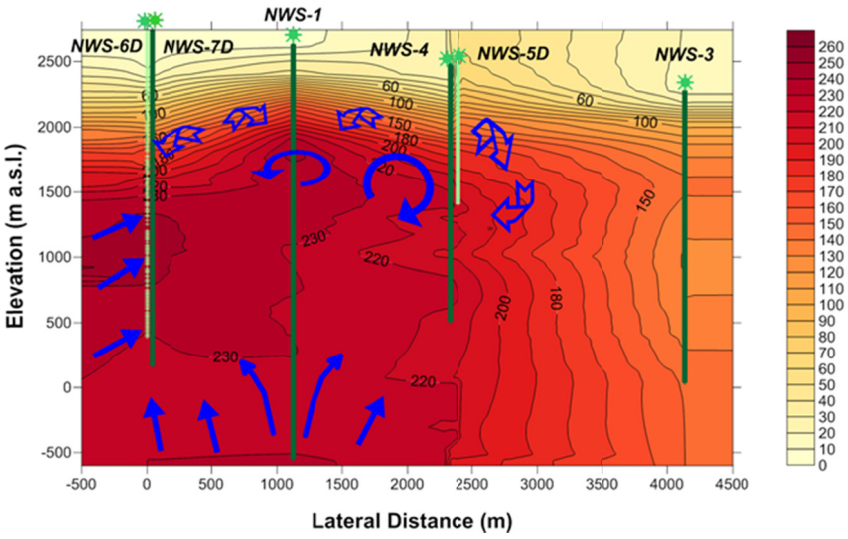

FIGURE 3: Temperature cross section of Sabalan geothermal field (Abdollahzadeh Bina, 2009)

Figure 4 shows the temperature logs of well NWS-6 at different times during heating and injection. Considering all the log measurements along with the latest surveyed spinner logs during shut in (Persia Energy Exploration Co., 2011), three main aquifers in the borehole with slightly different temperatures were identified:

a) *Aquifer 1* at depth 1138-1352.4 m, with average temperature of 204.5°C in injection test (2009) and average temperature of 233°C in heating-shut in test (2011);
b) *Aquifer 2* at depth 1467.5-1547.1 m, with average temperature of 238°C in injection test (2009) and average temperature of 231.5°C in heating-shut in test (2011);
c) *Aquifer 3* at depth 1690.5-2148.2 m, with average temperature of 237°C in injection test (2009) and average temperature of 230°C in heating-shut in test (2011).

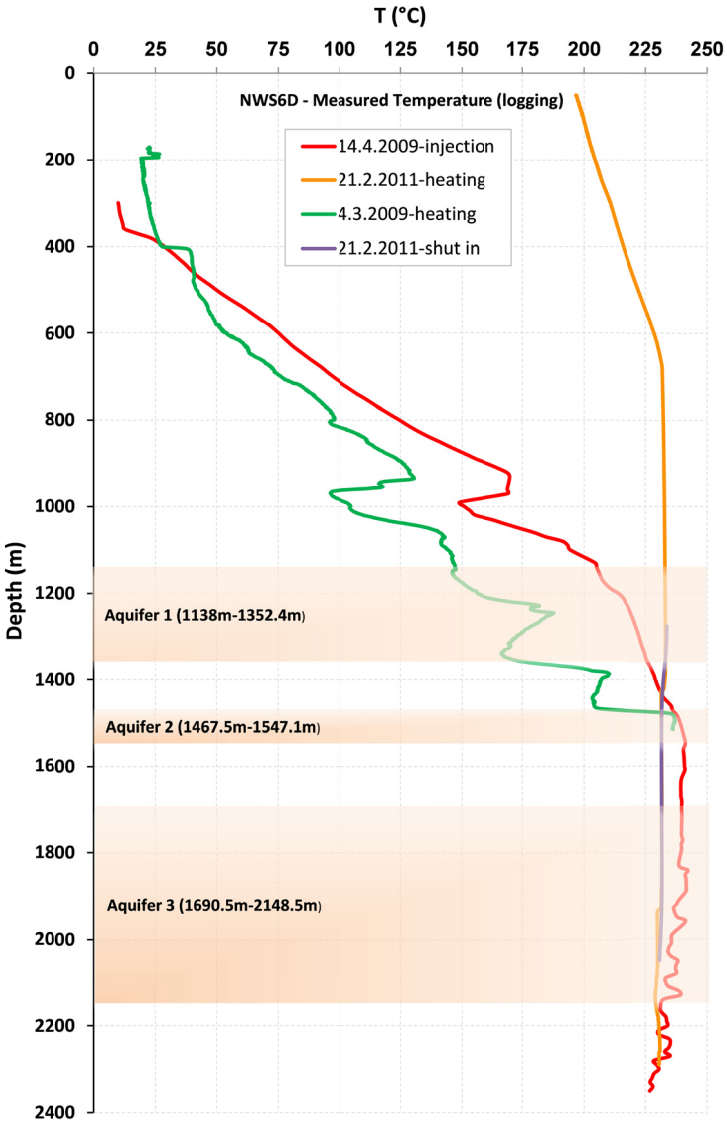

FIGURE 4: Downhole survey for well NWS-6D (modified from Abdollahzadeh Bina, 2009) and possible aquifers (Persia Energy Exploration Co., 2011)

Based on all the above mentioned studies, there is a good correspondence between temperatures estimated by logging, reservoir modelling and alteration minerals. Estimated temperatures deduced from alteration minerals in well NWS-7D (~240°C at 1534-1538 m) agree with the temperature survey results that recorded 241°C at 1540-1560 m depth. In addition, it seems that proposed aquifer 2 at 1467.5-1547.1 m is correlated with the assigned main feed zone, at 1485m (Abdollahzadeh Bina, 2009). The inverse temperature trends visible in the logging curves (Abdollahzadeh Bina, 2009) agree well with the inverse temperatures estimated by alteration minerals in NWS-7 at a depth of around 1320 m (~240-250°C) and 2180 m (≥250°C), and also for NWS-1 (1400-1500 m, 228°C; 2500-2900 m, 225°C). With regard to these results, an average temperature of 233°C seems to be reliable as the reference temperature for calculating the deep liquid chemical composition.

3.4 Chemistry of discharged fluids from NWS-1 and NWS-4

Based on SKM reports on discharged wells NWS-1 (2005b) and NWS-4 (2004b) and further interpretations by Rahmani (2007), the discharged fluid chemistry of wells NWS-1 and NWS-4 was classified as an alkaline-pH, medium salinity, sodium-chloride water. The discharged fluid was very analogous for most of the component concentrations except Ca, which in NWS-4 (25-30 ppm) is

double that in NWS-1 (15-30 ppm). In NWS-1, the Ca concentrations declined relative to Cl over the first week of discharging, possibly associated with calcite scaling in the wells or a high percentage of Ca bearing suspended solids in early samples. This evidence and the slight variation in other component concentrations of discharged fluid suggest that the initial water discharged from the wells may have derived from deeper and different inflow zones with relatively different composition, apparently with higher Ca concentration (Rahmani, 2007). The discharged steam chemistry of wells NWS-4 and NWS-1 is quite comparable. About 98% of the total gas content is CO_2, while H_2S, N_2, Ar, H_2 and CH_4 constitute the remaining steam components. Gas chemistry was reasonably stable throughout the discharge test with no significant changes in the response to well head pressure (WHP) changes or mass flow.

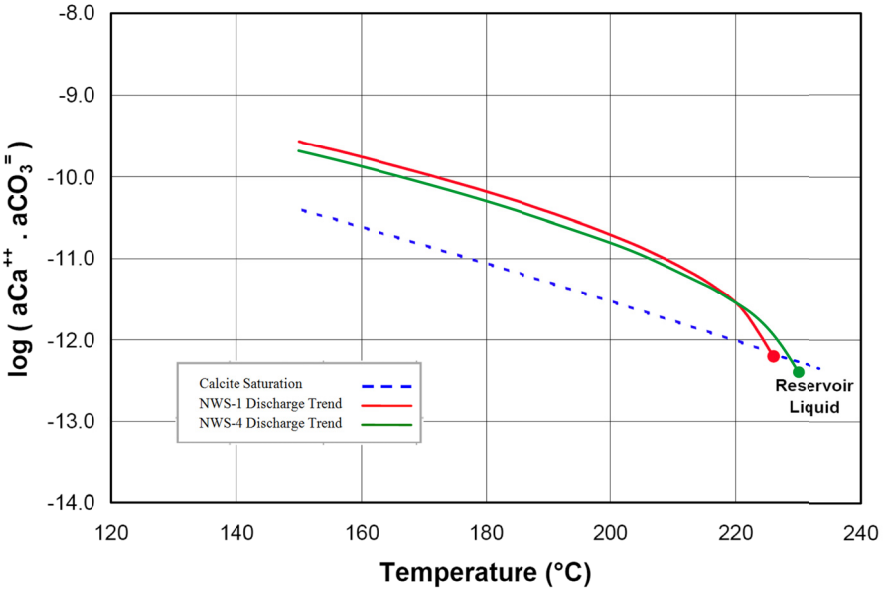

FIGURE 5: Simulation of calcite saturation in variably flashed water from wells NWS-1 and NWS-4 (SKM, 2004)

The chemical speciation of the reservoir liquids was calculated based on a reference temperature of 230°C. Calcite saturation was expected to be closely approached in the deep aquifers in Sabalan geothermal field (Rahmani, 2007). Taking into consideration the higher Ca concentration in deep liquid during the early days of discharging, the water was expected to be close to a calcite saturation state. It became significantly super-saturated when boiled and temperature decreased. At the end of the discharge test, the deep liquid was slightly but not significantly under-saturated. The calculated calcite saturation in the aquifer water of well NWS-4 was somewhat lower than that in well NWS-1 (Figure 5). This is considered to be a consequence of error in the calculated pH for aquifer liquid.

After discharging for two months, well NWS-1 choked because of calcite scaling. Well NWS-4 also stopped discharging abrubtly for unknown reasons with no sign of gradual pressure decline at the wellhead.

4. GEOCHEMICAL DATA INTERPRETATIONS

4.1 Sampling and analysis

Both good quality of analytical results and a sufficient quantity of liquid and steam samples are essential to gain a precise knowledge on the characteristics of geothermal reservoir fluids. They are also key to effectively solving reservoir management problems by providing valid information for evaluating reservoir behaviour through exploitation.

The data used in this report were made available by cooperation between SUNA and EDC´s on-site and office geochemists, experts and technicians. From a total of 24 samples, including 10

water samples and 14 steam samples, only 5 samples represent complete two-phase fluid samples. Steam samples were collected from a Webre separator on the wellhead, while the liquid samples were collected at both the weir box and the Webre separator on the wellhead. The assessed analytical data taken from well NWS-6D included Ca, Na, K, Mg, Li, Fe, Mn, B, Cl, F, SO_4, CO_2, H_2S, SiO_2, HCO_3, and NH_3 concentrations in the liquid phase, and CO_2 and H_2S in the gas phase. Tables 4 and 5 in Appendix I show the raw liquid and steam chemical data, respectively.

4.2 Results

Well NWS-6D was discharged for a period of about 142 days, from January to May, 2011. The average enthalpy was about 1250 kJ/kg while the discharge rates were variable: steam discharge increased from 22 to 55 t/hr while the water discharge varied between 60 and 140 t/hr. The separator pressure was set to be constant at 6 bar-g throughout the discharging days and also during water and steam sampling times (Appendix I, Table 3).

With the aid of the WATCH chemical speciation program, version 2.4, some of the important aspects such as calculated temperatures (geothermometers), chemical concentrations in the deep fluids at separator pressure (Appendix I, Table 1) and atmospheric pressure (Appendix I, Table 2) and the ionic balance were used to find the most appropriate analytical data to represent the real conditions of the deep aquifer. There were small discrepancies in the ionic balance data, ranging from -1.72 to -5.85%, that indicated an acceptable quality of thermal fluid analysis for speciation calculations. In addition, the relatively constant temperatures for each group of solute geothermometers (quartz and Na/K geothermometers) confirm the reliability of the analytical results.

4.3 Trends with time in the composition of well discharges

Appendix II shows the composition trends of the discharges. At first glance, it seems that there are some scatterings in the concentrations of components in specific samples, particularly samples taken on the 19^{th} and 40^{th} days of discharging. Sampling and analytical errors are unavoidable but, since nearly all the specific components with similar chemical behaviour in thermal systems changed approximately in the same way, even in the samples with exceptionally variable concentrations, it could be affirmed that not just sampling and analytical errors influenced the trends. Besides, with regard to the overall trends, concentration values and the restricted number of samples, the increase and decrease in some component concentrations were not as striking as first thought. Such fluctuations in some components, particularly soon after discharge initiation, could be related to the presence of more than one aquifer with slightly different fluid composition at depth. Similar rising trends of Na, Cl and B and declining trends of Fe and Mg in the water samples may be associated with both compositional variations of deep fluids through time and the different compositions of the aquifers.

The components measured in gas samples seem to be more scattered through time, but they are still relatively constant in concentration. The CO_2 concentrations range from 11300 to 26700 ppm and H_2S concentrations range from 54.4 to 313 ppm.

4.4 Correlation of discharge components with chloride

The concentrations of some components, such as B, SiO_2, Ca, Na, K and F, as a function of Cl concentration in the deep liquid for 5 two-phase analysed samples, are shown in Appendix III. These plots indicate that the chloride ratio is close to being linearly correlated with other components. A slight variation in ratio can imply more than one aquifer with different compositions in the well. Such variations are relatively constant for all plotted components, indicating the reliability of the analysis.

4.5 Cl-SO_4-HCO_3 ternary diagram

The Cl-SO_4-HCO_3 ternary diagram is one diagram for classifying natural waters based on the relative concentrations of the three major anions Cl^-, SO_4^{2-} and HCO_3^-. (Giggenbach, 1991). Chloride, which is a conservative ion in geothermal fluids, does not take part in reactions with rocks after it has dissolved. Its concentration is independent of the mineral equilibria that control the concentration of the rock-forming constituents. Thus, chloride is used as a tracer in geothermal investigations. Using this diagram, several types of thermal waters can be distinguished: mature waters, peripheral waters, steam-heated waters and volcanic waters. The diagram provides an initial indication of mixing relationships. According to Giggenbach (1991), chloride-rich waters are generally found near the upflow zones of geothermal systems. High SO_4^{2-} steam-heated waters are usually encountered over the more elevated parts of a field. The degree of separation between data points for high chloride and bicarbonate waters may give an idea of the relative degree of interaction of the CO_2 charge fluid at lower temperature, and of the HCO_3^- concentrations which increase with time and distance travelled underground.

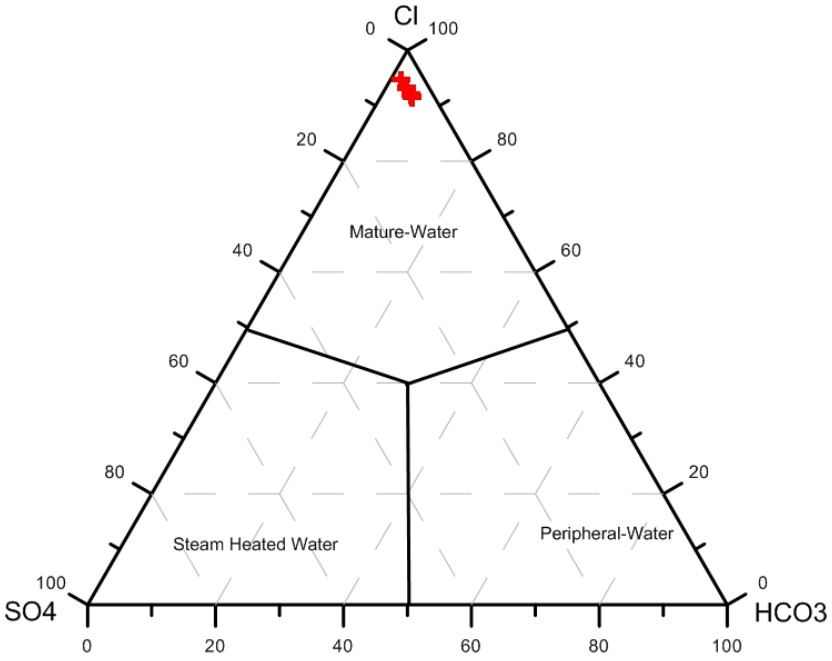

FIGURE 6: Comparative plot of relative Cl-SO_4-HCO_3 contents from the discharges of well NWS-6D

Figure 6 shows that all discharged water samples from NWS-6D well plot into the domain with high chloride mature waters. This is in agreement with previous geochemical studies in the area, including NWS-1, NWS-4 and springs. Concerning the relative abundance of chloride, sulphate and bicarbonate in the Sabalan wells, this water could be classified as a sodium-chloride type (SKM, 2004b and 2005b).

4.6 Geothermometry

Geothermometers are subsurface temperature indicators derived using the temperature dependent geochemical and/or isotopic composition of hot spring waters and other geothermal fluids under certain favourable conditions. The equilibrium between common minerals or mineral assemblages and a given water chemistry is temperature dependent. Many geochemists have observed that the relationship between chemical composition and temperature is predictable for certain parameters or ratios of parameters. Therefore, these parameters or ratios of parameters can serve as geothermometers. Geochemical and isotopic geothermometers rely on the following assumptions:

(i) There is equilibrium between liquid and minerals in the geothermal reservoir;
(ii) The activity or activity ratio is controlled predominantly by temperature; and
(iii) Re-equilibrium has not occurred during ascent and discharge (Gupta and Roy, 2007).

Therefore, the temperature indicated by the geothermometer is not necessarily the maximum temperature of the water, but the temperature at which mineral and water phases were last in equilibrium (Nicholson, 1993).

4.7 Solute geothermometers

In geochemical studies, the water chemistry and gas composition of geothermal fluids have proven useful in assessing the characteristics of geothermal reservoirs, both to estimate temperatures (Arnórsson and Gunnlaugsson, 1983) and to estimate initial steam fractions in the reservoir fluid (D'Amore and Celati, 1983; D'Amore and Truesdell, 1985). The following solute geothermometers were used in this study:

Quartz - Fournier (1977)
- Fournier and Potter (1982)

Na-K - Arnórsson et al. (1983)

4.7.1 Silica geothermometers

The increased solubility of quartz and its polymorphs at elevated temperatures has been used extensively as an indicator of reservoir temperatures (Fournier and Potter, 1982). Geochemical studies have shown that quartz is an important secondary mineral phase present and, therefore, it is common to compare the silica value of the thermal waters with the quartz solubility vs. temperature curve for deducing reservoir temperature. In systems above about 180°C, the silica concentration in the form of H_4SiO_4 is controlled by equilibrium with quartz. At lower temperatures, equilibrium with chalcedony becomes important. One of the assumptions made in such calculations is that silica dissolved at high temperature at depth remains metastable in the solution and does not precipitate as the thermal waters rise to the surface. This is mostly true when the fluid discharge is considerable and water rises rapidly, which is what happens with high-temperature well discharge (Gupta and Roy, 2007). The solubility reactions for silica minerals can be expressed as:

$$SiO_{2,solid} + 2H_2O = H_4SiO_4^o \quad (1)$$

However $H_4SiO_4°$ is not only an aqueous silica species in natural waters. $H_4SiO_4°$ is a weak acid which dissociates, if the pH of the fluid is high enough to yield $H_3SiO_4^-$.

$$H_4SiO_4^o = H^+ + H_3SiO_4^- \quad (2)$$

Analysis of silica in an aqueous solution yields the total silica concentration, generally expressed as ppm SiO_2, which includes both un-ionized $H_4SiO_4°$ and ionized ($H_3SiO_4^-$). The dissociation constant for silicic acid is about 10^{-10} at 25°C. It means that the quartz geothermometers are valid for the sample with pH lower than 10. Since the maximum pH of the samples was 7.6, all the silica concentrations in the samples were undissociated silicic acid and the quartz geothermometer was valid for the samples.

At a pH of 10 ($[H^+] = 10^{-10}$), the concentration of unionized silica equals that of ionized silica:

$$K_{H_4SiO_4°} = \frac{[H^+][H_3SiO_4^-]}{[H_4SiO_4^o]} \quad (3)$$

The quartz geothermometers used to estimate the aquifer temperatures in this report are the following:

Fournier (1977)

$$t\,(°C) = \frac{1309}{5.19 - \log S} - 273.15 \quad (4)$$

Fournier and Potter (1982)

$$t(°C) = -42.2 + 0.28831S - 3.6686 \times 10^{-4}S^2 + 3.1665 \times 10^{-7}S^3 + 77.034 \log S \quad (5)$$

where S refers to SiO_2 concentrations, such as in deep liquid, in mg/kg. The results for the quartz thermometer are presented in Table 2. Accordingly, the average temperature for the deep aquifer

using the quartz geothermometer equation of Fournier (1977) is 232.3°C. The quartz geothermometer, using the equations of Fournier and Potter (1982) yields a temperature of 234.2°C. These temperatures correspond well with quartz temperatures calculated by WATCH (234°C).

4.7.2 Cation geothermometer

A common geothermometer used where geothermal waters are known to come from high-temperature environments is the ratio of sodium to potassium (Na/K). The ratio decreases with increasing temperature. The cation concentrations (Na^+, K^+) in a solution are controlled by temperature-dependent equilibrium reactions with feldspars (albite and K-feldspar) that have often been described as exchange reactions. The main advantage of this thermometer compared to the quartz geothermeter is that it is relatively unaffected by dilution and provided that the dilution involves relatively dilute groundwaters. The Na/K geothermometer is also immune to steam separation (Gupta and Roy, 2007). The exchange reaction is expressed as:

$$NaAlSi_3O_8 + K^+ = KAlSi_3O_8 + Na^+ \quad (6)$$

The equilibrium constant, $K_{eq,}$ for reaction 6 is:

$$K_{eq} = \frac{[KAlSi_3O_8][Na^+]}{[NaAlSi_3O_8][K^+]} \quad (7)$$

The activities of the minerals are assumed to be unity and the activities of the dissolved species are about equal to their molal concentrations in aqueous solution. Equation 7 reduces to:

$$K_{eq} = \frac{[Na^+]}{[K^+]} \quad (8)$$

In this report the equation suggested by Arnórsson et al. (1983) for temperatures in the range of 250-350°C, was used for calculating reservoir temperatures based on the Na/K activity ratio in the geothermal fluid:

$$t(°C) = \frac{1319}{1.699 + \log(Na/K)} - 273.15 \quad (9)$$

As presented in Table 2, the average temperature of the thermal aquifer deep in well NWS-6 is 268.5°C; that corresponds well with the calculated Na-K thermometer of 265.7°C (by WATCH). This temperature may represent the source body of the thermal aquifer at deeper levels. There is some discrepancy between the quartz and Na/K temperatures. It is commonly observed that Na/K temperatures are higher than quartz temperatures. This might occur by the influence of other equilibria (i.e. albite and K-feldspar not controlling the Na/K ratio); the other common explanation is that the Na/K equilibrium re-equilibrates slower than quartz and, thus, has a more valid temperature for the deep liquid temperatures, i.e. higher temperatures at deeper levels in the system.

4.8 Gas geothermometers

In many high-temperature geothermal fields (> 200°C), the gas content of geothermal discharges (fumaroles and wells) like CO_2, H_2S, H_2, N_2, NH_3, and CH_4 , has been used to obtain information on the source of the fluid and its temperature. Gas geothermometers may be used on the assumption of specific gas-gas or mineral-gas equilibria and/or the distribution of isotope ratios between gaseous species (Arnórsson et al., 2007). They include both gas concentrations and gas ratios or a combination of ratios. The calibration of gas geothermometers, based on thermodynamic data, rests on an assumption of specific chemical equilibria. It means that, for each specific chemical equilibrium, a thermodynamic equilibrium constant may be expressed in terms of temperature; thus, the concentration of each gas species is often represented by its partial pressure in the vapour phase (D'Amore and Truesdell, 1985). This assumption needs to be verified by comparing gas

geothermometer results with solute or isotope geothermometers and especially with well temperature data.

When using gas geothermometry, it is important to keep in mind that several factors other than aquifer temperature may affect the gas composition of a geothermal fluid. In geothermal reservoir fluids, gas concentrations at equilibrium depend on the ratio of steam to water in that fluid, whereas the gas content of fumarole steam is also affected by the boiling mechanism in the upflow, steam condensation and the separation pressure of the steam from the parent water. Furthermore, the flux of gaseous components into geothermal systems from their magmatic heat source may be quite significant and influenced by how closely gas-gas and mineral-gas equilibria are approached in specific aquifers (D'Amore and Arnórsson, 2000). In this study, the gas geothermometers used are those based on gas concentrations in mmol/kg corrected to the atmospheric pressure.

As formerly explained, all of the NWS-6D well steam samples were collected from the Webre separator which is connected to the two-phase pipeline discharging into the atmospheric silencer. The WATCH chemical speciation program assumes that both liquid water and steam samples are collected at the same pressure, while the sample which is collected at the separator pressure has a smaller steam fraction than the sample collected at atmospheric pressure. In order to use the gas geothermometer, the effect of further boiling, from separator pressure to atmospheric pressure should be taken into account. Assuming that all the gas is in the steam fraction:

$$X^s \cdot m^s = X^a \cdot m^a \tag{10}$$

Here, X^s is the steam fraction at the separator pressure, X^a represents the steam fraction of the well discharge at atmospheric pressure, m^s represents the gas concentration in the steam sample that is collected from the Webre separator, and m^a represents the gas concentrations in the steam sample that could be collected in atmospheric conditions. To find the gas concentration in a steam sample at atmospheric pressure:

$$m^a = m^s \left(\frac{X^s}{X^a}\right) \tag{11}$$

The geothermometers are based on mineral gas equilibria for the following reactions:

$$2Ca_2Al_3Si_3O_{12}(OH) + 2CaCO_3 + 3SiO_2 + 2H_2O = 3Ca_2Al_2Si_3O_{10}(OH)_2 + 2CO_{2,aq} \tag{12}$$

$$FeS_2 + FeS + 2Ca_2Al_2Si_3O_{10}(OH)_2 + 2H_2O = 2Ca_2Al_2FeSi_3O_{12}(OH) + 3H_2S_{aq} \tag{13}$$

Q in the gas geothermometry equations represents the gas concentrations in log mmol/kg. The equations are:

For TCO_2 (Arnórsson et al., 1998b):

$$T(°C) = 4.724Q^3 - 11.068Q^2 + 72.012Q + 121.8 \tag{14}$$

For TH_2S (Arnórsson and Gunnlaugsson, 1985) that can be applied for all the waters in the range of 200-300°C and Cl > 500 ppm:

$$T(°C) = 246.7 + 44.8\,Q \tag{15}$$

A gas geothermometer of H_2S is well correlated with a Na-K geothermometer, while a CO_2 geothermometer shows higher temperatures than all the other gas and solute thermometers. It can be explained by the high CO_2 concentrations in the deep liquid.

TABLE 2: Various solute and gas geothermometers of well NWS-6D, Sabalan

Days	Sampling date	Solute geothermomters (°C)			WATCH-T (°C)		Gas geothermo-meters (°C)		T_{ref}
		T_{q-1}	T_{q-2}	T_{NaK}	T_Q	T_{NK}	T_{CO2}	T_{H2S}	
8	14.01.11	235.4	238.1	264.9	237.9	261.5	283.7	259.8	**233**
27	02.02.11	233.4	233.0	270.8	232.9	268.3	308.1	261.1	**233**
30	05.02.11	233.4	235.9	270.4	235.3	267.9	306.9	274.3	**233**
40	15.02.11	230.9	233.2	267.4	233.1	264.4	303.2	271.8	**233**
51	26.02.11	228.5	230.6	269.0	231	266.4	300.8	249.6	**233**
T_{av} (°C)		**232.3**	**234.2**	**268.5**	**234.0**	**265.7**	**300.5**	**263.3**	**233**

T_{q-1} Fournier (1977); T_{q-2} Fournier and Potter (1982);
T_{NaK} Arnórsson et al. (1983); T_Q WATCH calculated quartz;
T_{NK} WATCH calculated Na-K; T_{CO2} Arnórsson (1998);
T_{H2S} Arnórsson and Gunnlaugsson (1985) $T_{av.}$ Average temperature
T_{ref} Observed temperatures;

5. SCALING POTENTIAL AND SCALE INHIBITION METHODS

Precipitation of solid scales from geothermal fluids is the most problematic issue in the utilization of geothermal resources. Solid scaling occurs as mineral deposition from the boiling fluid in reaction to its cooling and degassing in upflow zones of geothermal systems and in wells with substantial boiling (Arnórsson et al., 2007). According to Corsi (1986), scale deposition can be divided into three main types including: deposition from a single phase fluid (injection pipelines); deposition from flashing fluid (wells, separators, two phase-pipelines); and deposition by steam carry-over (separators, steam lines and turbines).

Amorphous silica (the non-crystalline form of silica) and carbonates (calcite and aragonite) are generally the most troublesome scales in wells but metallic sulphides may also cause problems at high temperatures where concentrations of dissolved solids are high (Hardardóttir et al., 2001). Both amorphous silica and carbonate scales are white coloured and not visually easy to tell apart. The silica scales often appear grey or black due to small amounts of iron sulphide, a corrosion product found inside all geothermal pipelines. A quick method to distinguish these is to put a drop of hydrochloric acid on a piece and, if bubbles are formed, it is calcite. In terms of solubility, these scales show reverse characteristics, i.e. contrary to anhydrite, calcite and aragonite with retrograde solubility (solubility decreases with increasing temperature); silica and metallic sulphides have prograde solubility with temperature increase (Thorhallsson, 2005). When cooling takes place, minerals with prograde solubility, therefore, would be over-saturated in geothermal fluids and those with retrograde solubility would become under-saturated. The solubility of calcite, aragonite and metallic sulphides is also controlled by pH; therefore, they become over-saturated in geothermal waters during degassing (Arnórsson et al., 2007). In other words, temperature and pH together with the rate of the precipitation reaction play important roles in determining whether or not the minerals with which the water becomes over-saturated precipitate from solution. The degree of over-saturation, fluid composition and kinetics of the precipitation reaction are other factors affecting the amount of minerals precipitated from solution (Arnórsson, 2000).

5.1 Silica scaling potential

It has been established that aqueous silica concentrations in high-temperature geothermal fluids are controlled by a close approach to equilibrium with quartz (Gunnarsson and Arnórsson et al., 2000).

Silica scales are found to some extent in all geothermal installations but, by maintaining the temperature above the solubility level for amorphous silica, the scaling rate stays very low; this is one of the design criteria for most geothermal plants. The silica concentration in the water increases at the same time as solubility decreases through boiling and cooling down the water. The water immediately becomes quartz supersaturated, but no quartz precipitates are formed because of the slow formation of quartz crystals. It is known in practice that only some 25% of the water can be converted into steam without the danger of silica scales. In other words, it is only possible to cool the water by some 100°C without silica scaling. Thus, reservoir water of 240°C must be separated above 140°C in order to avoid silica scaling. For this reason, it is not of greatest importance that the reservoir temperature be as high as possible since silica scale formation becomes more problematic at higher temperatuers. The higher the reservoir temperature, the higher the temperature of the separated water needs to be. Therefore, amorphous silica heads the list of scaling problems associated with the reinjection of waste water (Thorhallsson, 2005). Deposition of silica in and around the wellbore causes a reduction in formation permeability and, subsequently, the injectivity of the well (Hauksson and Gudmundsson, 1986).

Five two-phase analysed samples (samples # 8, 27, 30, 40 and 51, Table 2, Appendix I) were used to evaluate the silica saturation state of the deep liquid phase in well NWS-6D. Figure 7 shows how the saturation state of silica (quartz and amorphous silica) in the liquid changes during adiabatic boiling, based on a reference temperature of 233°C. This reference temperature was deduced from logging measurements in the well and estimated temperature by alteration minerals in the formation and introduced to WATCH 2.4 to calculate aquifer composition, the consequent activity product (Q) and the equilibrium constant (K) of reaction 1. Figure 7 shows that the deep liquid has a super-saturation state with amorphous silica at temperatures lower than around 118°C and with quartz in temperatures lower than around 232°C. Consequently, silica is not a big problem in the surface pipelines and power plant of Sabalan geothermal field.

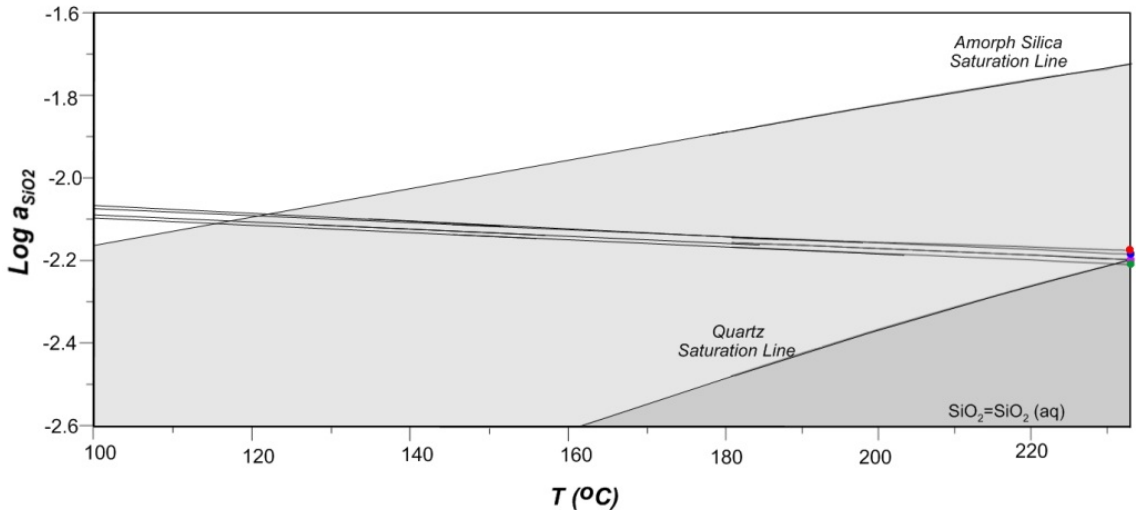

FIGURE 7: Silica saturation during boiling of fluid from NWS-6D (ref. temperature = 233°C)

5.2 Coping with silica scaling

Although there is no single standard solution to all silica scaling problems, the basic rule is that silica precipitation rate is slowed down by low pH and low temperature (even though the degree of supersaturation is higher) and this is often taken advantage of in the process design (Angcoy Jr., 2006). Similarly, the silica precipitation rate is positively correlated with the total concentration of dissolved solids. Among several methods adapted to reduce or eliminate deposition of amorphous silica in production wells and wellhead equipment, the commonly adapted method is to maintain steam separation pressures (and temperatures) above amorphous silica saturation. In the case of

Sabalan geothermal field, this limit of the injected water temperature is about 125°C; thus the temperature of injected waters into the wells should not be lower than 125°C. Using this method, called the "hot injection" method, waste water from geothermal production wells is pumped from steam separators to the injection wells. This practice limits the amount of heat that can be extracted from the fluid discharged from the production wells. Another common method to prevent silica scaling is pumping the waste water from conditioning ponds after it has cooled down or been treated such that the silica has polymerized. The method deemed most favourable for each operation is a function of (a) the reservoir temperature, and (b) the water salinity or the overall water composition. These are also acceptable disposal methods from geological and environmental points of view. By the first method, "hot injection", contact with the atmosphere is avoided. For water disposed of on the surface (second method), methods of fluid disposal include: (a) direct infiltration; (b) polymerization of the silica in special conditioning ponds followed by conveyance of the treated water to infiltration ponds; (c) evaporation in large disposal ponds; (d) storage in effluent ponds where the silica polymerizes and the polymers subsequently settle by gravity before allowing the water to infiltrate; and (e) chemical treatment of the water involving the removal of silica from solutions by using acids (Asaye, 2004).

5.3 Calcite scaling

Many researchers have reported that calcium carbonate (in the crystalline forms of calcite or aragonite) is a major scale-forming mineral in many geothermal systems. According to Ocampo-Diaz et al. (2005), calcite deposition is subject to salinity, pH and the concentration of calcium and dissolved CO_2 in the deep liquid. Unboiled geothermal liquids at reservoir conditions are typically close to being calcite-saturated (Arnórsson, 1989). Calcite precipitates from brines according to the following reaction:

$$Ca^{2+}(aq) + 2HCO_3^- \leftrightarrow CaCO_3(s) + H_2O + CO_2 \quad (16)$$

Calcite would be deposited when there is CO_2 loss from the liquid phase into a gas phase (degassing) upon flashing (rapid conversion of water into steam) and causes this reaction to be forced to the right. The extent of degassing and cooling determines whether boiling causes an initially calcite saturated water to become over or under-saturated (Arnórsson et al., 2007).

Calcite scales are common in wells of reservoirs that have temperatures in the range of 140-240°C. Calcite scales are usually primarily found over a 200-300 m long section in the well above where flashing occurs, but are not found so much below or above that section. At higher reservoir temperature the quantity of dissolved calcite in the water will be less and, therefore, calcite scaling is usually not a problem in wells that produce from reservoirs with a higher temperature than 260°C. At temperatures above 300°C, especially in highly saline water, more complex minerals can form scales, mainly metal sulphides, silicates and oxides (Thorhallsson, 2005).

Four two-phase analysed samples (samples # 27, 30, 40 and 51, Table 2, Appendix I) were used to evaluate the calcite saturation state of the deep liquid phase in well NWS-6D during adiabatic boiling. Figure 8 indicates that the deep liquid is super-saturated at temperatures lower than the reference temperature of 233°C and under-saturated at temperatures above 233°C. This reference temperature is deduced from logging measurements in the well and estimated temperature by alteration minerals in the formation; it is then introduced to WATCH 2.4 to calculate the aquifer composition, consequent activity product (Q) and the equilibrium constant (K) of reaction 1. Different samples in quartz temperatures show insignificantly different temperatures of the reservoir fluid, ranging from 229°C to 234°C (Figure 9). This range of temperature for the boiling temperature of the aquifer corresponds well with the observed reference temperature of 233°C. Accordingly, the deep liquid can be considered to be super-saturated with calcite at temperatures lower than 229°C. An unrealistic state of

geothermal reservoir solutions, when applying a Na-K thermometer (Figure 10), supports the reliability of the reference temperature of 233°C being used for deep liquid calculations.

5.4 Coping with calcite scaling

Three main methods have been applied to cope with calcite scaling (Pieri et al., 1989). One involves making the water calcite-undersaturated, either by the addition of acid or CO_2 (Kuwada, 1982). Another method involves periodic mechanical cleaning and the third uses inhibitors (Crane and Kengeremath, 1981). Mechanical cleaning or the use of inhibitors are the most commonly applied remedies.

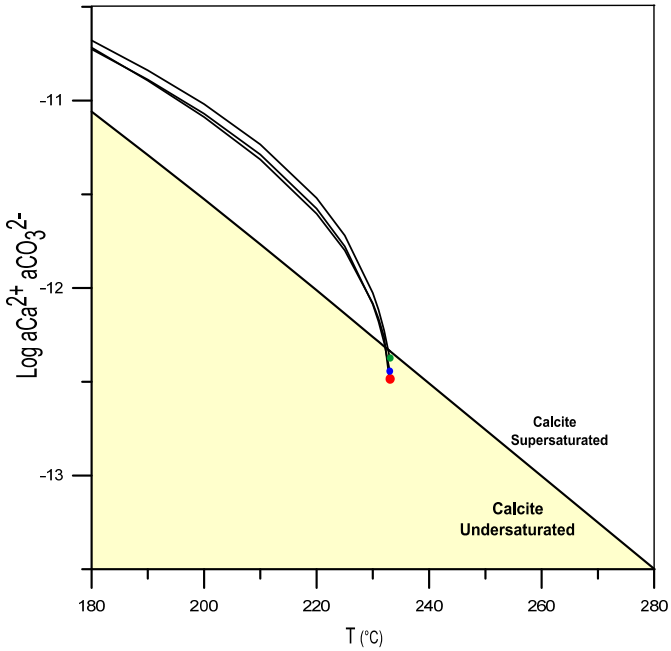

FIGURE 8: Calcite saturation during boiling of fluid from NWS-6D (ref. temperature = 233°C)

5.4.1 Mechanical cleaning of the well

The most successful mechanical cleaning method involves drilling out the scale with a small truck-mounted rig while the well is being produced. Using this method, the scale is brought to the surface, thus not accumulating at the well bottom. A cleaning operation takes one to two days to be completed and then the well can be immediately connected. This method does not involve cooling down the well before cleaning, thus avoiding extra strains on the casing and cement. In a case of unavoidable cooling, and to minimize thermal strain on the pipes, cooling the well must be moderated and the temperature and the flow rate of the water must be gradually increased or decreased. This method is feasible if the deposition is not very fast and if cleaning is required no more than about twice a year. If scale formation is faster, the use of scale inhibitors is a more beneficial method. It is important to keep in mind that the cleaning operations of the wells must use an economically acceptable method (Asaye, 2004).

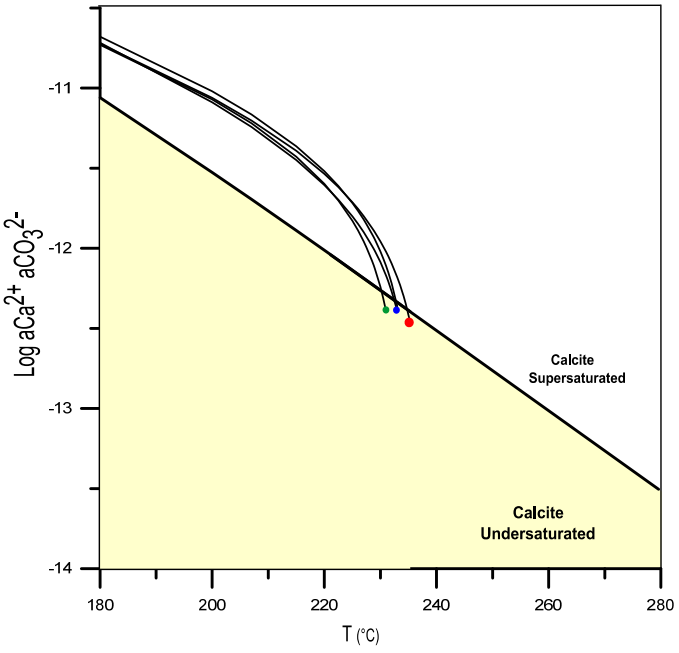

FIGURE 9: Calcite saturation during boiling of fluid from NWS-6D. Reference temperature is taken to be equal to quartz temperature as computed by WATCH

This method can be successful if the deposits are formed inside the production casing. In a study carried out on geothermal scaling, scale thickness ranged from 0.7 to approximately 3 cm and resulted in costly fluid restriction of 10-45% (Vetter, 1987). Reaming of the well in the casing section will recover the original output fully. However, if the deposits are formed in the slotted liner and the slots, the deposits cannot be cleaned completely by reaming. In this case, side tracking may be the only

option. In order to determine the location and thickness of scales in geothermal wells, different mechanical methods are used. These methods include: a) using wire baskets of different diameters, lowered on a logging wire until it stops, and b) a caliper logging tool that is an electrical logging tool with four arms. The disadvantage of the caliper tool is the temperature limitation of the electronics. Thus, in order to use the caliper logs, the well should be cooled down, which causes a negative effect on well casings and the cement structure due to straining. Usually the well needs to be killed and cooled down for a caliper survey; while using wire baskets, the measurements can be done in the flowing well (Molina, 1995).

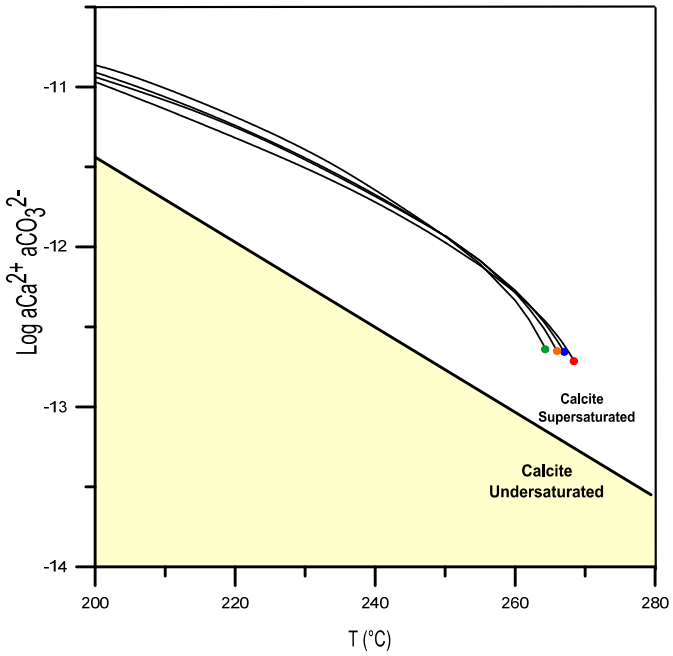

FIGURE 10: Calcite saturation during boiling of fluid from NWS-6D. Reference temperature taken to be equal to the Na/K temperature computed by WATCH

The method shown in Figure 11 was developed for the cleaning operation in the wells of the Svartsengi geothermal field in Iceland. The results obtained by this method have been very favourable as the wells have been cleaned 31 times, recovering the original output every time. The method includes the following steps (Molina, 1995):

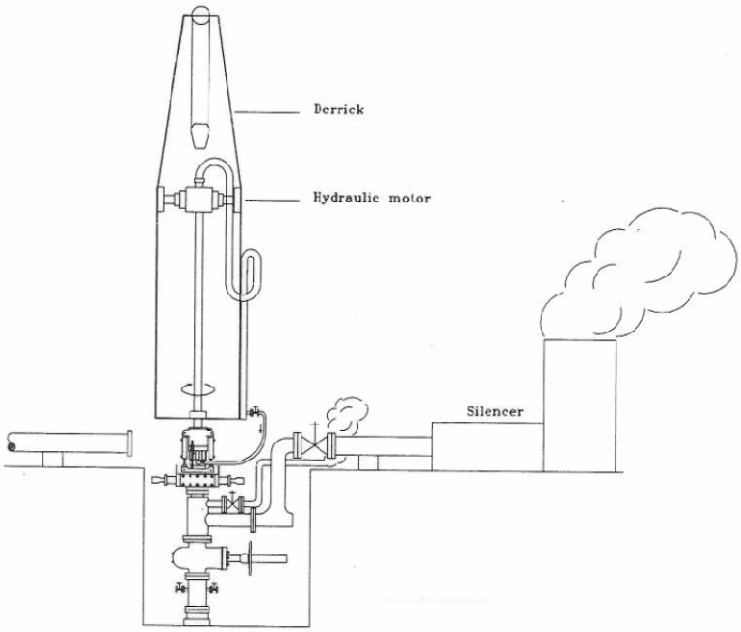

FIGURE 11: Cleaning operation in a discharge well in Iceland (Molina, 1995)

a. The well is in normal production, but should be cleaned;
b. Close master valve and remove wellhead assembly;
c. Hoist gland and bit into position. Bitsub has metal to metal return valve or is blanked;
d. Move the rig over the well and connect first drill collar. Master valve is closed;
e. Open master valve and pull-in drillpipe to overcome pressure in well until the drill string is heavy enough;
f. Reaming of scaling from the well. No water circulation, only flow from the well;
g. Trip-out with the flow line valve closed after cleaning the well.

5.4.2 Chemical treatment of the well

Chemical treatment of geothermal water, either with an acid (commonly hydrochloric acid or sulphuric acid) or CO_2, to make the calcite become undersaturated has been successfully applied in recent years. This method is known to rejuvenate the permeability in injection wells, most likely

because the acid dissolves the acid soluble mineral, probably calcite that has precipitated from the injection water as a result of its heating in the formation (Arnórsson, 1995). This indicates that acid leaching, together with cold reinjection may be the best methods to cope with calcite deposition from reinjected geothermal water. The lower the temperature of the reinjected water and the lower the temperature of the receiving formation, the smaller the chances that the water will attain calcite saturation. This method has, however, several disadvantages. Due to the relatively high pH buffer capacity of geothermal waters, a large amount of acid may be required, making this treatment expensive and, therefore, not attractive economically (Arnórsson, 1995).

Further, acidification may render the water corrosive which has adverse effects on downhole casing, surface pipeworks, installations and the environment (Asaye, 2004). For decreasing the effects of corrosion, it is better to not use high yield-strength steel for casing and liner during the drilling stage of exploration. Therefore, using a casing type of K-55 or L-80 run in high-temperature cement is among the best alternatives. In addition, Cr-steel might be needed for the uppermost 100 m of casing. For surface installations, it is better to use mild steel for steam pipes, while a super-heated steam pipe should be isolated. Scrubbing such pipes manually might also effectively decrease corrosion. For condensate pipelines, stainless steel, fiberglass and polypropylene plastic are applicable. If a geothermal solution contains high Cl^- concentrations, it is recommended to use a titanium alloy in the heat exchanger (Asaye, 2004).

Using CO_2 instead of acid is challenging, too; as the CO_2 partial pressure of the main geothermal fluids is usually very high, large quantities of CO_2 may have to be added to make the reservoir water significantly calcite undersaturated, especially after it has flashed. The process and instruments for applying the acidization method are the same as for the calcite inhibitor system which are described in the next section (Corsi, 1986) (Figure 12).

5.4.3 Calcite inhibitor system (CIS)

The inhibition of calcite scale deposits by using chemical products has gained importance, both technically and economically, and seems to be one of the most promising systems. This method is beneficial economically when scale formation is so fast that the well needs to be cleaned more than twice a year (Pieri et al., 1989). In this section, a combination of information, achieved by experience in calcite inhibitor system components, instruments, inhibitors and operation process in three producing geothermal fields, is briefly described. These fields include Miravalles geothermal field, Costa Rica (Moya and Nietzen, 2010), Leyte geothermal production field, Philippines (Siega et al., 2005) and Mindanao geothermal production field, Philippines (Nogara et al., 2000).

Basically, this method consists of running a coiled tube into the well and setting it at the desired depth. For an effective inhibition, the chemical inhibitor has been dosed traditionally about 50 to 100 m below the flash point. Arrangements for inhibition are very similar in different geothermal wells. Figure 12 shows the schematic diagram of the calcite inhibition system installed in

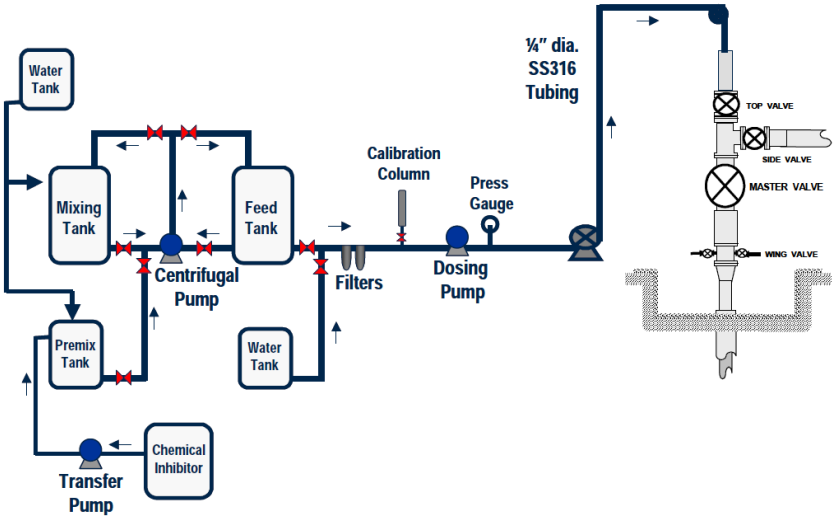

FIGURE 12: Schematic diagram of the surface injection facility for the calcite inhibition system (Siega et al., 2005)

Mindanao geothermal production field (MGPF), Philippines. In some cases, it is necessary to previously remove the scale mechanically. The main problem encountered with downhole injection is the corrosion of the injection pipe by the inhibitor. This problem can be solved by using an injection pipe made of a suitable corrosion-resistant alloy (Piere et al., 1989).

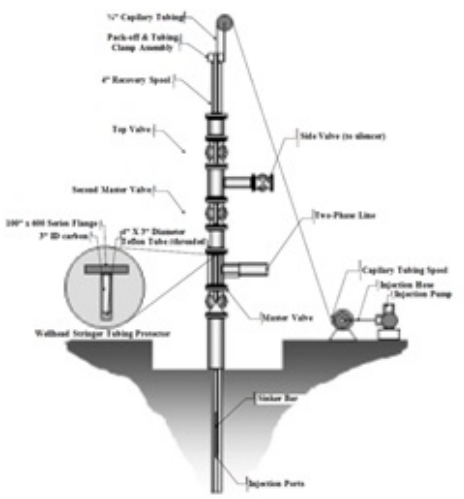

FIGURE 13: Schematic of the calcite system installed in well SP4D, Philippines (Nogara et al., 2000)

The calcite inhibitor system consists of: (a) surface feed equipment (production well inhibitor storage and pumping system) (Figure 12), and (b) down-hole injection system (production well inhibitor downhole feed system) installed through the wellhead (Figures 12 and 13). The surface feed system is made up of an inhibitor storage tank (2000-L high-density polyethylene), two ⅓-HP chemical dosing pumps (one of them as reserve), calibration pot and pressure gauges. The injection system consists of a stuffing box, lubricator, hay pulley, weight bar (sinker), chamber and capillary tubing and drum.

A 0.25-inch outer diameter (0.18 inch inner diameter) capillary tube is weighted down with a sinker bar and a dispersion head set at the borehole. Capillary tubing for injection at depth is a considerably sensitive part of the system. The selection of their diameter and material should be compatible with the volume to be injected, the chemical product to be used and the temperatures to be exposed, otherwise it can suffer attacks which would originate obstructions and ruptures. For example, as the inhibitors may change phase when exposed to high temperatures for long times (become jelly-like), the tubing may get choked. The length of the capillary tubing ranges between 1,100 and 1,500 m, and the material is an alloy of 316 L. The weight bar (sinker bar) helps to stabilize the components as well as lift and lower the inhibition head. Weight calculations must be made for successful retrenchment of the tubing with the chamber. A 3-inch stinger pipe can be set above the master valve to prevent the tubing from being sucked into the production tree. To protect the tubing from rubbing against the stinger, a teflon tube can be introduced at the bottom of the stinger. A stuffing box at the surface pack-off on top of the recovery spool is able to prevent leakage of geothermal fluids to the environment. Braided teflon inside the pack-off would protect the tubing from rubbing against the metal surface. The type of material used in the inhibitor injection system must be designed so as to resist corrosion, high temperature and pressure. One of the important factors influencing corrosion is the chemical composition of the fluid. Therefore, when choosing the system, the material most suitable to the specific field conditions must be investigated.

Other main structural elements of a calcite inhibition system include:

- *Electrical supply support system* – it guarantees a constant operation of the dosing pumps and the different on-line monitoring elements. The required reliability degree depends on the scaling velocity in the well, so that with a high scaling rate the electrical supply quality in operation can play a crucial role.
- *Storage tank* – The material for the storage tank must be chemically inert with respect to the inhibitor used. Experience has shown that any high density polyethylene container is a good option. The tanks or places where they are located should have prevention and contention systems for spills, for fulfilling all the environmental norms.
- *Injection pump* – the market offers a great diversity, but not all of them are qualified for working in long periods of time under the working pressures required and the aggressiveness of the chemical used. The injection capillary tube‘s inner diameters (3.95 mm) and its longitude (1500 meters) pose another problem; the pumps must have fine mesh filters.

- *Inserting and fastening elements* – necessary components to ease the introduction, withdrawal and fastening of the capillary tubing inside the well. The designing objective is not only the functionality but the ease and security of these procedures, which can take from 1 to 2 hours. It should have pulleys with appropriate diameters for not causing unnecessary fatigue to the capillary tubing, which could lead to premature failure or a rupture.

The choice of a suitable inhibitor and the system for injecting it into the well is critical. The most common types of inhibitors currently in use today for calcite scale control include polyacrylic acid (PAA) and polymaleic anhydrides (PMA). Both types of inhibitors are acidic in nature, of the carboxylic acid (COOH) functional group (Ramos-Candelaria, 1999). The PAAs have a straight chain with one COOH in the monomer, while the PMAs have a ring for the monomer with 2 COOH groups (Figure 14). Organic phosphate esters, organic phosphates, organic synthetic polymers (e.g. polyacrylamide), organic polymers (e.g. polyacarboxylic acids), sequetering agents (e.g. EDTA) and polyphosphates (successful in low temperature situations) are the other types of inhibitors in use today. Nalco 1340 HP (high purity) has been used in geothermal wells in Iceland successfully (personal communication with S. Thorhallsson, 2011). It is an effective inhibitor but at a 5% concentration ratio, it precipitated due to bacterial growth and polymerization of the inhibitor. It was a perfect application when used at a 10% concentration ratio and mixed with deionized water. Table 3 shows some common inhibitors used in Krafla geothermal field, Iceland. In Miravalles geothermal field, Costa Rica, different types of inhibitors have been tested including Nalco 1340 HP Plus, Geosperse 8410CN Plus and BWA DP 3537. Nalco 9354 and BetzDearborn DG9349 inhibitors have been used successfully in MGPF wells, Philippines (Table 4). These inhibitors were technically assessed with respect to their (a) thermal stability using the NACE test, (b) percent inhibition by their ability to keep Ca^{2+} in solution, and (c) field tests. These chemicals also had the lowest prices among the anti-scalants considered.

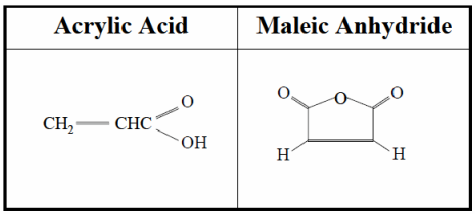

FIGURE 14: Chemical structures of common base units (Siega et al., 2005)

TABLE 3: List of calcite inhibitors used in Krafla geothermal field, Iceland (Ármannsson, 2011)

Trade name	Composition	Conc. ratio (%)	Price (USD/kg)
Dequest 2006	Aminotori (methylene phosphate acid) 38-40%	2-10	1.35
Nalco95D0666	Polymaleic acid 30-60% - Maleic acid 1-5%	1-5	4.95
Nalco 1340 HP	Polyacrylate	2-10	4.95
Drewsperse747A	Polycarboxylic acid 40-55% (Acrylic copolymer)	0.5-10	4-5

TABLE 4: List of calcite inhibitors used in production fields of MGPF, Philippines

Inhibitor	Type	Effective conc.
N9354	Polyacrylates	5 ppm
DG9349	Polymaleic Anhydride	2 ppm

The mechanisms of chemical inhibition usually include the prevention of precipitated scale crystals from adhering to surfaces and thereby distorting the crystal to keep it from growing in a precise geometric pattern by developing negative charges in the water. In addition, a large negative charge is imparted on the aborted micro-crystals causing them to repel other like particles. The net effect is that very small non-adherent crystals are formed which can be easily swept away by fluid flows. The selected inhibitor must preserve its resistance when subjected to high temperatures.

Inhibitor storage and distribution steps can be described as follows:

- Reception of the inhibitor (pure product) at the dilution plant and then verification, quantification and storage in 50,000 kg tanks;
- Dilution of the pure inhibitor and water to different concentrations, depending on the pumping system and on the recommended dosage at the dilution plant;
- Distribution of the diluted inhibitor to the various storage tanks located at the wells. A cistern can be used to distribute the inhibitor in each well in the geothermal field.

5.4.4 Monitoring of CIS

In this section, a combination of information, obtained by experience in calcite inhibitor system components, instruments, inhibitors and operation process in two producing geothermal fields, is briefly described. These fields include Miravalles geothermal field, Costa Rica (Moya and Nietzen, 2010) and Mindanao geothermal production field, Philippines (Nogara et al., 2000). Various geochemical and physical parameters should be monitored during the inhibition trial. Physical parameters or operating parameters include: well head pressure (WHP), weight of downhole injection system, injection pressure of dosing pump, bore output (waterflow, steamflow and enthalpy) of the well, simulated flash point depths and inhibitor injection flow rates. The injection pressure of the dosing pump or pumping pressure is important for detecting possible problems in the capillary tubing, such as partial or total obstruction inside the capillary tubing, or broken tubing. The pump capacity must be selected in a flexible manner to be able to adopt changing well production rates. Inhibitor injection flow rates can be measured by two parameters including: a) consumption time that is defined as the time it takes a column of 100 ml of inhibitor to be injected into the well (T100), indicating the rate of inhibitor flow, and b) inhibitor level in the tank (m). Generally, it is more beneficial that the calcite inhibition system composes an automated monitoring system for a healthy inhibitor injection operation (for example in case of pump failure, decreasing inhibitor level in the storage tanks, etc.).

Geochemical parameters include water and steam chemistry, a calcite saturation index (CSI), and inhibitor concentrations. To monitor these parameters, pH, Ca, Cl and HCO_3^- concentrations should be determined by periodic sampling and analysis of the thermal fluid of the well. In Miravalles geothermal field, Costa Rica, samples are taken weekly at each well to verify the effectiveness of the inhibitor, and if it is found that the bicarbonates have changed, then further studies are carried out to adjust the inhibitor‘s dosage. As the Cl concentration is constant in the producing or discharging fluid, achieving a constant ratio of Ca/Cl indicates the effectiveness of the inhibition process. If any parameter is out of range, a corrective action is taken to adjust the system to normal conditions. Both a short turnaround time for analyses and the order of the data processing are important for achieving a fast determination.

Monitoring the chemical and hydraulic evolution of the field is useful for determining and tracking changes that can affect the performance of a calcite inhibition system, especially those related to the working dosage and the inhibitor‘s injection depth. The field tests usually begin with an inhibitor overdosage, and then when the calcium values under total inhibition conditions are found, the dosage is lowered until optimum values are determined. In other words, if when reducing the inhibition doses the calcium values lower, it means that the well is under-dosed and this will generate a partial scaling of the well. In well PGM-49 of Miravalles geothermal field, Costa Rica, an initial dosage of 0.50 ppm of inhibitor was needed, but at present it needs a dosage of 2.5 ppm. In other wells in this field, the behaviour has been just the opposite; the inhibitor consumption can either increase or decrease with time. The injected inhibitor concentration versus calcium concentration of the fluid should be continuous to ensure that the required effective concentration of the inhibitor of the well discharge fluids is maintained. This method is called the ‘threshold‘ method. The threshold dosage of inhibitors in Iceland is ~4 mg/kg (personal communication with Sverrir Thórhallsson, 2011).

5.4.5 Economic considerations in using calcite scaling methods

In this section, the cost of most common methods used for calcite scaling control, including chemical inhibition systems and the mechanical cleanout in Miravalles geothermal field, Costa Rica, (Moya and Nietzen, 2010) and Kizildereh geothermal field, Turkey (Kaya et al., 2010) is briefly reviewed. The purpose of using chemical treatment systems in geothermal production wells is to allow for commercial exploitation of the wells (Moya and Nietzen, 2010).

a. Miravalles geothermal field, Costa Rica

The inhibition system lengthens the lifetime of the well, as well as its production periods, without the need to carry out frequent mechanical cleanouts. The initial investment in Miravalles geothermal field was a little more than a million and a half dollars ($1,528,124) for the inhibition system in a field with 5 producers, and an annual cost of $205,203 which includes depreciation, operation and maintenance costs. On average, a well without an inhibition system could produce for only 3 months at the Miravalles geothermal field.

Comparing two options for removing the calcite scales with or without a calcite inhibition system (considering a total of 5 wells with an average output of 7 MW per well) shows that, most likely, more than one mechanical cleanout would be required per well per year but, if the conservative assumption resulted in a higher net cost than the use of the calcite inhibition system for a production period of a year, then the calcite inhibition system would always be cheaper than mechanical cleanouts in wells that require one or more mechanical cleanouts in a year (Table 5). Without an inhibition system, the productivity of the wells would decline over time, until their wellhead pressures would be too low to allow their integration to the gathering system. It may be possible to operate wells without calcite scale inhibition systems, instead withdrawing them from production periodically when they require cleaning. Even when this option is possible, it has several disadvantages, such as loss of production during the mechanical cleanout periods, production decline over time, and possible further damage to the formation near the wellbore, among others. To produce the well again, a drilling rig would be required to perform a mechanical cleanout. This creates additional costs, such as equipment, personnel and the generation lost during the cleanout period which, on average, lasts for 15 days.

TABLE 5: Parameters for comparison of scale control options
in Miravalles geothermal field, Costa Rica (Moya and Nietzen, 2010)

			Value	Unit
Parameter	**Well**	Average generation per well	7	MW
		Average price of energy delivered (2003)	0.04113	$/kWh
		Total wells integrated to the system	5	
	Mechanical cleanouts	Mechanical cleanout average cost	136.233	$
		Average costs, operation & maintenance before and after mechanical cleanout	10.042	$
		Average time for cleanout	15	Days
	Process without CIS	Estimated time without inhibition	350	
		Decay rate of the well	0.028	MW/day

The cost of energy not produced is the most significant item; this is calculated by subtracting the energy produced by a well without an inhibition system from the energy produced by a well with an inhibition system over a given period of time. The energy delivered by the well without an inhibition system is reduced due to two main factors: (a) the decline in output over time due to obstruction by calcite, and (b) the energy not produced during the mechanical cleanout. If one estimates 15 days for a mechanical cleanout, then during the remaining 350 days, more energy would be delivered by the well with the inhibition system than by the well without the inhibition system, due to the decline caused by wellbore scaling. From another point of view, the main cost saving comes from eliminating lost production, since there would be no need to withdraw the well from production for a mechanical

cleanout. There is also the benefit of increasing the well's lifetime, by avoiding possible damage to the inside of the wellbore during a mechanical cleanout.

b. Kizildereh geothermal field, Turkey

Scale formation has direct influence on the amount of steam supplied to the power plant since the productivity of the wells may decline 70-75% in 8-9 months in Kizildereh geothermal field. Furthermore, shutting down a well for mechanical cleaning also creates additional loss of steam provided to the power plant. In order to test the cost-effectiveness of constructing an inhibitor injection system, a simple cash flow analysis for two different cases of geothermal fluid production (production with inhibitor injection and production without inhibitor injection) was performed for a period of 10 years. In the case of electricity production without inhibitor injection to the wells, an acidizing operation was performed every 10 years, and mechanical reaming was done every year. In the case of electricity production with inhibitor injection to the wells, an acidizing operation would be performed once in the life of the system, while mechanical cleaning would be done every 5 years (Kaya et al., 2010). It is anticipated that, even if an inhibitor was injected into the wells, there still might be some slight loss due to scaling. Therefore, a yearly production decline rate of 4% was assumed. It was observed that utilization of an inhibitor system in Kizildereh geothermal field created an increased profit of approximately $14 million over a 10 year period. On the other hand, the utilization of an inhibitor would stabilize the electricity generation at a steady level, and a cumulative amount of electricity generated would show a noteworthy trend compared to electricity generation with mechanical cleaning of the wells (Figure 15). So test studies proved that the application of an inhibitor injection system as a preventative measure is an effective approach in terms of both achieving continuous electricity generation and cost effectiveness.

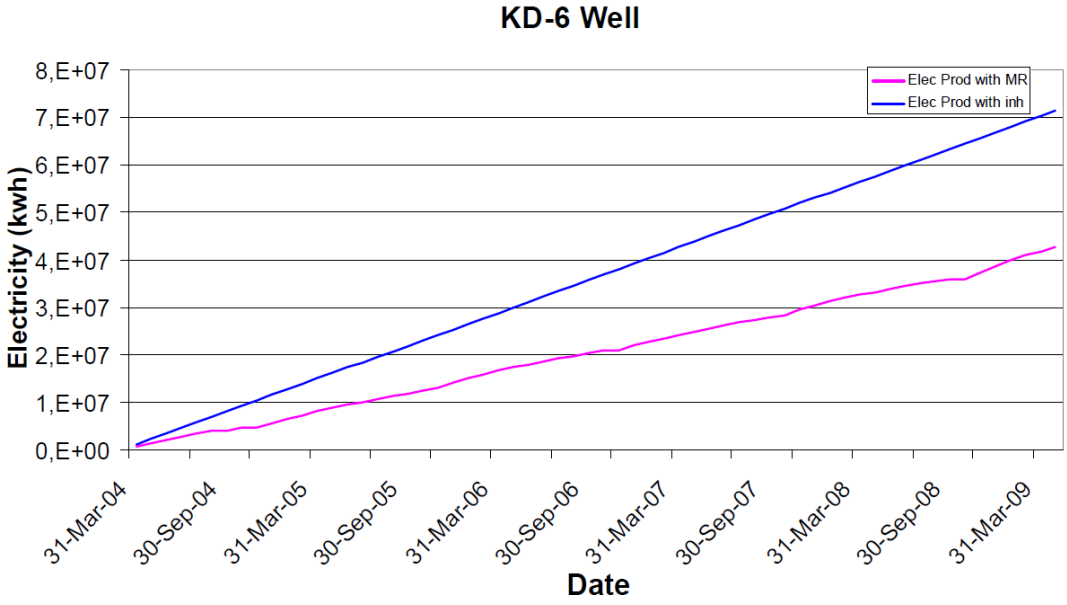

FIGURE 15: Comparison of cumulative electricity generation with and without inhibitor injection in Kizildereh geothermal field, Turkey (Kaya et al., 2010)

6. CONCLUSION AND RECOMMENDATIONS

The main outputs of the interpretation of chemical data of discharged fluids from wells NWS-6D are:

- Variation in component concentrations in discharged fluids correlated with time and Cl concentration is probably a result of the presence of more than one aquifer in the deep levels with slightly different fluid compositions.

- Quartz geothermometers gave an average temperature of 233°C for deep liquid in the well. There was a good correspondence between temperatures estimated by quartz geothermometers and temperatures estimated by logging, reservoir modelling and alteration minerals at different reservoir depths. Na-K geothermometers gave an average temperature of 268°C and H_2S geothermometers gave an average temperature of 263°C for deeper levels of the reservoir.
- Silica scaling will not be a serious problem if the injected water temperature is not allowed to be lower than 125°C before it is injected, as the deep liquid is in a super-saturated state with amorphous silica at temperatures of about 118-125°C.
- Calcite scaling will be the main problem in the production wells as the deep liquid is very close to calcite saturation under reservoir conditions.

Regarding the prospect of Sabalan geothermal field and also common methods used in other geothermal fields in the world, a calcite inhibitor system (CIS) is economically and technically the best alternative to preventing calcite scaling in the wells and allowing continuous production. Mechanical cleaning methods can be more beneficial when the wells should be discharged just for sampling and reservoir assessments (not for electricity production) for long periods of time, if the economic and technical aspects of available shallow rigs are manageable.

To improve the quality of the Sabalan reservoir geochemical model, some recommendations can be made:

- At least 10 two-phase discharged fluid samples should be collected simultaneously and then analysed precisely and accurately for both steam and liquid phases;
- Wells NWS-6D, NWS-7D and NWS-10D (located in the same drilling pad) can be considered typical wells to geochemically assess the Sabalan reservoir;
- Wells NWS-6D, NWS-7D and NWS-10D can be considered typical wells in the Sabalan geothermal field for installation of a calcite inhibitor system and for finding a practical operational procedure for the wells in the production stage of the project;
- Economic and technical aspects of mechanical cleaning and chemical treatment methods should be meticulously evaluated to cope with calcite scaling in the discharge test stage and later production stage, depending on the project scheme.

ACKNOWLEDGEMENTS

I would like to express my deepest gratitude to Dr. Ingvar B. Fridleifsson, Director, and Mr. Lúdvík S. Georgsson, Deputy Director of the United Nation University, Iceland, for giving me the opportunity to attend the UNU Geothermal Training Programme in 2011. I am sincerely grateful to my supervisor, Dr. Thráinn Fridriksson for his valuable discussions and comments during my work on the report. Furthermore, thanks go to Ms. Thórhildur Ísberg, Mrs. Dorthe H. Holm and Mr. Markús A.G. Wilde for their help. I would also like to give thanks to Mr. Armoodli, Managing Director of SUNA - the Renewable Energy Organization of Iran, Dr. Ramezani, Deputy Managing Director of SUNA, and Dr. Porkhial, the Sabalan Geothermal Project Director for supporting me during these 6 months. I am also grateful to the staff members of the Sabalan geothermal project for their technical support.

Last, but definitely not least, I'm very grateful to my family, especially my wife, Mastaneh Haghnazar Liseroudi, for support, patience and encouragement throughout my stay in Iceland.

REFERENCES

Abdollahzadeh Bina, F., 2009*:* Northwest Sabalan geothermal resource assessment through well testing. Report 6 in: *Geothermal training in Iceland 2009.* UNU-GTP, Iceland, 15-44.

Angcoy Jr., E.C., 2006: An experiment on monomeric and polymeric silica precipitation rates from supersaturated solutions. Report 5 in: *Geothermal Training in Iceland 2006.* UNU-GTP, Iceland, 21-50.

Ármannsson, H., 2011: *Fluid chemistry and utilization.* UNU-GTP, Iceland, unpublished lecture notes.

Arnórsson, S., 1989: The use of gas chemistry to evaluate boiling processes and initial steam fractions in geothermal reservoirs with examples from Suswa field, Kenya. *Geothermics, 19,* 497-514.

Arnórsson, S., 1995: Scaling problems and treatment of separated water before injection. In: Rivera, J. (editor), *Injection technology.* World Geothermal Congress 1995, IGA pre-congress course, Pisa, Italy, 65-111.

Arnórsson, S. (ed.), 2000: *Isotopic and chemical techniques in geothermal exploration, development and use. Sampling methods, data handling, interpretation*. International Atomic Energy Agency, Vienna*,* 351 pp.

Arnórsson, S., Fridriksson, T., and Gunnarsson, I., 1998: Gas chemistry of the Krafla geothermal field, Iceland. *Proceedings of the 10th International Symposium on Water-Rock Interaction, Balkema, Rotterdam*, 613-616.

Arnórsson, S., and Gunnlaugsson, E., 1983: Gas chemistry in geothermal systems. *Proceedings of the 9th Workshop on Geothermal Reservoir Engineering, Stanford University, Stanford, CA*, 231-237.

Arnórsson, S., and Gunnlaugsson, E., 1985: New gas geothermometers for geothermal exploration-Calibration and application, *Geochim. Cosmochim. Acta, 49,* 1307-1325.

Arnórsson, S., Gunnlaugsson, E., and Svavarsson, H., 1983: The chemistry of geothermal waters in Iceland III. Mineral equilibria and independent variables controlling water compositions. *Geochim. Cosmochim. Acta, 47,* 547-566.

Arnórsson, S., Stefánsson, A., and Bjarnason, J.Ö., 2007: Fluid-fluid interaction in geothermal systems. *Reviews in Mineralogy & Geochemistry, 65,* 259-312.

Asaye, M., 2004: Methods to evaluate flow and scaling in geothermal systems with reference to the case: Aluto Langano Power Plant, Ethopia*.* Report 3 in: *Geothermal Training in Iceland 2004.* UNU-GTP, Iceland, 1-24.

Bjarnason, J.Ö., 2010: *The speciation program WATCH, Version 2.4, user's guide.* The Iceland water chemistry group, Reykjavik, 9 pp.

Bogie, I., Cartwright, A.J., Khosrawi, K., Talebi, B., and Sahabi, F., 2000: The Meshkin Shahr geothermal prospect, Iran. *Proceedings of the World Geothermal Congress 2000, Kyushu-Tohoku, Japan,* 997-1002.

Corsi, R., 1986: Corrosion and scaling in geothermal fluids. *Geothermics, 15,* 94 -96.

Crane, C.H., and Kengeremath, D.C., 1981: *Review and evaluation of literature on testing of chemical additives for scale control in geothermal fluids*. U.S. DOE, report DOE/1D/12183-P, 90 pp.

D'Amore, F., and Arnórsson, S., 2000: Geothermometry. In: Arnórsson, S. (editor), *Isotopic and chemical techniques in geothermal exploration, development and use. Sampling methods, data handling, and interpretation.* IAEA Vienna, 152-199.

D'Amore, F., and Celati, C., 1983: Methodology for calculating steam quality in geothermal reservoirs. *Geothermics, 12,* 129-140.

D'Amore, F., and Truesdell, A.H., 1985: Calculation of geothermal reservoir temperatures and steam fractions from gas compositions. *Geothermal Resources Council Transactions, 9,* 305-310.

EDC, 2009a: *Petrology of well NWS-7D, Northwest Sabalan, Iran*. EDC, report for SUNA - Renewable Energy Organization of Iran, 27 pp.

EDC, 2009b: *Petrology of NW Sabalan cores: Wells NWS-6D, NWS-7D, NWS-5RD.* EDC, report for SUNA - Renewable Energy Organization of Iran, 12 pp.

ENEL, 1983: *Geothermal power development studies in Iran.* ENEL, general report to the Ministry of Energy, Iran, 168 pp.

Faridi, M., 2010: *Structural geology of Mount Sabalan.* SUNA - Renewable Energy Organization of Iran, report, 62 pp.

Fournier, R.O., 1977: Chemical geothermometers and mixing model for geothermal systems. *Geothermics, 5,* 41-50.

Fournier, R.O., and Potter, R.W.II., 1982: A revised and expanded silica (quartz) geothermometer. *Geothermal Reources Council Bulletin, 11-10,* 3-12.

Giggenbach, W.F., 1991: Chemical techniques in geothermal exploration. In: D'Amore, F. (coordinator), *Application of geochemistry in geothermal reservoir development.* UNITAR/UNDP publication, Rome, 119-142.

Gunnarsson, I., and Arnórsson, S., 2000; Amorphous silica solubility and the thermodynamic properties of H_4SiO_4 in the range of 0°C to 350°C at P sat. *Geochim. Cosmochim. Acta, 64,* 2295-2307.

Gupta, K., and Roy, S., 2007: *Geothermal energy, an alternative resource for the 21th century.* Elsevier, NY, 293 pp.

Hardardóttir, V., Kristmannsdóttir, H., and Ármannsson, H., 2001: Scale formation in wells RN-09 and RN-08 in the Reykjanes geothermal field, Iceland. *Proceedings of the 10th International Symposium on Water-Rock Interaction, Villasimius, Italy, Balkema, Rotterdam*, 851-854.

Hauksson, T., and Gudmundsson, J.S., 1986: Silica deposition during injection in Svartsengi field. G*eothermal Resources Council Transactions, 10,* 377-384.

Kaya, T., Demirci, N., Kaya, R., Alpagut Bükülmez, A., Dedeoğlu, V., 2010: Economical aspects of the scale inhibitor injection system operation. *Proceedings of the World Geothermal Congress 2010, Bali, Indonesia,* 4 pp.

Kuwada J.T., 1982: Field determination of EFP system for carbonate scale control. *Geothermal Reources Council, Bulletin, 11,* 3-6.

McKenzie, D.P., 1972: Active tectonics of Mediterranean region. *Geophys. J.R. Astron. Soc.,30-2,* 109-185.

Molina Argueta, G.G., 1995: Rehabilitation of geothermal wells with scaling problems. Report 9 in: *Geothermal Training in Iceland 1995.* UNU-GTP, Iceland, 207-240.

Moya, P., and Nietzen, F., 2010: Performance of calcium carbonate inhibition and neutralization systems for production wells at the Miravalles geothermal field. *Proceedings of the World Geothermal Congress, Bali, Indonesia,* 10 pp.

Nicholson, K., 1993: *Geothermal fluids: Chemistry and exploration techniques.* Springer Verlag, Berlin, 263 pp.

Nogara, J.B., Ramos-Candelaria, M.N., Esberto, M.B., Buñing, B.C., Trazona, R.G., and Cabel Jr., A.C., 2000: *Calcite inhibition in well SP4D, Mindanao geothermal production field (MGPF), Philippines*. PNOC, Energy Development Corporation, 8 pp.

Noorollahi, Y., Jamaledini, M.R., and Ghazban, F., 1998: *Geothermal potential areas in Iran.* Renewable Energy Organization of Iran, 175 pp.

Ocampo-Díaz, J.D., Núñez, Q.M., and Moya-Acosta, S.L., 2005: Silica scaling as a predominant factor of the production in Cerro Prieto geothermal wells, Mexico. *Proceedings of the World Geothermal Congress 2005, Antalya, Turkey,* 5 pp.

Persia Energy Exploration Co., 2011: *On-site interpretation.* PEECo, report for SUNA – Renewable Energy Organization of Iran, 7 pp.

Pieri, S., Sabatelli, F., and Tarquini, B., 1989: Field testing of downhole scale inhibitor injection, *Geothermics, 18,* 249-257.

Ramos-Candelaria, M.N., 1999: Survey of chemical inhibitor applications for controlling calcite deposition in geothermal wells. *Proceedings of the 20th Annual PNOC-EDC Geothermal Conference, Philippines*.

Shadkam Torbati, S., 2007: Numerical reservoir modelling of the Sabalan geothermal field, NW Iran. *Proceedings of the 10th International Geothermal Conference, Auckland, New Zealand,* 48 pp.

Siega, F.L., Herras, E.B., and Buñing, B.C., 2005: Calcite scale inhibition: The case of Mahanagdong wells in Leyte geothermal production field, Philippines. *Proceedings World Geothermal Congress 2005 Antalya, Turkey,* 6 pp.

Rahmani, M., 2007: Assessment of calcite scaling potential in the geothermal wells in NW- Sabalan prospect, NW-Iran. Report 19 in: *Geothermal Training in Iceland 2007.* UNU-GTP, Iceland, 447-460.

SKM, 2003: *Geological report for well NWS-1*. Sinclair Knight Merz, report for SUNA – Renewable Energy Organization of Iran, 206 pp.

SKM, 2004a: *Geological report for well NWS-4.* Sinclair Knight Merz, report for SUNA – Renewable Energy Organization of Iran, 278 pp.

SKM, 2004b: *Well NWS-4 geochemical evaluation report.* Sinclair Knight Merz, report for SUNA – Renewable Energy Organization of Iran, 22 pp.

SKM, 2005a: *NW-Sabalan geothermal feasibility study.* Sinclair Knight Merz, report for SUNA – Renewable Energy Organization of Iran, 140 pp.

SKM, 2005b: *Geochemical evaluation of well NWS-1.* Sinclair Knight Merz, report for SUNA – Renewable Energy Organization of Iran, 19 pp.

SKM, 2005c: *Extended geological mapping at the northwest Sabalan geothermal project.* Sinclair Knight Merz, report for SUNA – Renewable Energy Organization of Iran, 60 pp.

TB, 1979: *Geothermal power development studies, Sabalan Zone.* Tehran Berkeley, report to the Ministry of Energy, Iran.

Thórhallsson, S., 2005: Common problems faced in geothermal generation and how to deal with them. *Presented at Workshop for Decision Makers on Geothermal Projects and Management, UNU-GTP and KengGen, Naivasha, Kenya,* 12 pp.

Vetter, J.M., 1987: Test and evaluation methodology for scale inhibitor evaluation. *International Symposium on Oilfield Chemistry, San Antonio, Texas, SPE paper 16259*, 159-186.

APPENDIX I : Water and gas analysis and deep fluid concentrations in well NWS-6D, Sabalan

TABLE 1: Deep fluid concentration at separator pressure (ppm)

		Liquid sample													Gas sample		
Days	**Date**	**SiO_2**	**B**	**Na**	**K**	**Ca**	**Mg**	**SO_4**	**Cl**	**F**	**Fe**	**CO_2**	**H_2S**	**NH_3**	**CO_2**	**H_2S**	**NH_3**
8	**14.01.11**	557.5	24.1	1650.5	291.9	14.9	0.19	104.8	2820	5.13	0.11	49.7	1.2	0.13	6683	59.4	1.53
27	**02.02.11**	527.9	23.2	1552.9	291.9	11.9	0.21	99.6	2649	5.0	0.18	55.8	7.6	0.15	11636	553.4	1.5
30	**05.02.11**	544.8	22.7	1528.7	286.2	11.9	0.3	100	2625	0.19	0.19	47.2	1.4	0.24	11335	118.5	2.7
40	**15.02.11**	528.7	23.4	1596.5	289.6	12.2	0.24	101.9	2707	5.1	0.2	46.9	1.4	0.22	10449	105.2	2.1
51	**26.02.11**	513.8	21.6	1581.6	291.9	12.9	0.22	95.1	2634	4.9	0.15	40.5	0.5	0.34	9971	42.6	3.1

TABLE 2: Deep fluid concentration at atmospheric pressure (ppm)

		Liquid sample													Gas sample	
Days	**Date**	**pH**	**SiO2**	**B**	**Na**	**K**	**Ca**	**Mg**	**SO4**	**Cl**	**F**	**Fe**	**CO2**	**H2S**	**NH3**	**CO2**	**H2S**
8	**14.01.11**	6.0	405.8	17.5	1199.4	212.1	10.9	0.14	76.2	2050	3.8	0.08	1951	17.8	1951	258	2.7
27	**02.02.11**	5.7	383.4	16.9	1128.4	212.1	8.7	0.15	72.4	1925	3.7	0.13	3377	17.8	3377	452	2.9
30	**05.02.11**	5.7	395.9	16.5	1110.8	208	8.7	0.22	70.2	1908	0.14	0.14	3284	34.9	3284	440	5.7
40	**15.02.11**	5.8	384.2	17.0	1160.1	210.4	8.8	0.17	74.1	1968	3.7	0.16	3030	31	3030	406	5.0
51	**26.02.11**	5.7	373.3	15.7	1149.3	212.1	9.3	0.16	69.1	1914	3.5	0.11	2886	12.2	2886	384	1.6

TABLE 3: Physical properties of discharging well NWS-6D

			Physical properties				
No	**Days**	**Date**	**pH**	**pH T**	**GSP (bar)**	**WHP (bar)**	**Enth. (kJ/kg)**
1	3	09.01.11	8.46	21.10	6	12.5	1246
2	4	10.01.11	8.51	23.15	6	12.5	1305
3	8	14.01.11	7.65	13.20	6	12.5	1126
4	10	16.01.11	7.50	16.50	6	12.5	1408
5	19	25.01.11	8.63	16.80	6	12.8	1150
6	23	29.01.11	6.82	17.90	6	10	1150
7	27	02.02.11	6.86	20.10	6	11.5	1257?
8	28	03.02.11	6.73	16.80	6	11.5	1257
9	30	05.02.11	6.57	17.30	6	11.5	1152
10	31	06.02.11	6.67	11.80	6	11.5	1215
11	32	07.02.11	6.55	19.90	6	11.5	1222
12	40	15.02.11	6.84	16.40	6	9.8	1182
13	51	26.02.11	6.45	22.80	6	12.5	1258
14	101	17.04.11	8.51	26.40	6	12.5	1258
15	124	10.05.11	6.52	20.50	6	10.5	1252
16	131	17.05.11	6.66	21.00	6	9.8	1269
17	138	24.05.11	6.80	21.00	6	9.8	1269
18	142	28.05.11	6.91	21.80	-	-	-

TABLE 4: Water analysis of fluids from well NWS-6D

			Water analysis (ppm)								
No	**Days**	**Date**	**Al**	**Li**	**Na**	**K**	**Ca**	**Mg**	**Fe**	**Mn**	**Cl**
1	3	09.01.11	1.51	8.70	1444.70	255.71	13.52	0.15	0.09	0.02	2432.22
2	4	10.01.11	1.47	8.64	1423.48	255.78	12.92	0.16	0.13	0.02	2411.53
3	8	14.01.11	1.76	8.70	1436.00	254.00	13.00	0.17	0.10	<0.02	2454.00
4	10	16.01.11	1.76	8.64	1439.00	256.00	12.90	0.18	0.16	<0.02	2450.00
5	19	25.01.11	1.48	8.78	1477.41	265.18	11.11	0.27	0.31	0.02	2452.02
6	23	29.01.11	1.76	8.44	1362.00	248.00	10.40	0.22	0.18	<0.02	2322.00
7	27	02.02.11	1.76	8.49	1351.00	254.00	10.40	0.18	0.16	<0.02	2305.00
8	30	05.02.11	1.76	8.21	1330.00	249.00	10.40	0.26	0.17	<0.02	2284.00
9	40	15.02.11	1.76	8.55	1389.00	252.00	10.60	0.21	0.19	<0.02	2356.00
10	51	26.02.11	1.76	7.83	1376.00	254.00	11.20	0.19	0.13	<0.02	2292.00

			Water analysis (ppm)									
No	**Days**	**Date**	**B**	**SiO_2**	**HCO_3**	**CO_3**	**tCO_2**	**H_2S**	**SO_4**	**NH_3**	**F**	**EC**
1	3	09.01.11	20.75	484.72	85.06	4.11	64.40	2.00	91.26	0.56	4.47	8460
2	4	10.01.11	20.79	480.77	87.26	3.42	65.27	2.29	90.68	0.66	4.41	8500
3	8	14.01.11	21.00	485.00	124.00	ND	97.70	3.12	91.20	0.58	4.46	7490
4	10	16.01.11	21.00	487.00	121.00	ND	96.20	3.63	91.70	0.60	4.53	7500
5	19	25.01.11	21.27	487.30	43.05	2.01	32.54	0.91	93.84	0.65	4.71	-
6	23	29.01.11	20.40	464.00	126.00	ND	116.00	2.62	88.20	1.21	4.48	-
7	27	02.02.11	20.20	459.00	125.00	ND	122.00	2.74	86.70	0.59	4.38	
8	30	05.02.11	19.80	474.00	124.00	ND	115.00	3.45	84.10	0.90	4.31	
9	40	15.02.11	20.40	460.00	123.00	ND	106.00	3.50	88.70	0.82	4.45	
10	51	26.02.11	18.80	447.00	123.00	ND	124.00	3.89	82.70	1.23	4.24	

TABLE 5: Gas analysis of fluids from well NWS-6D

No.	**Days**	**Date**	**Gas analysis (ppm)**	
			CO_2	**H_2S**
			mmol per 1 mole steam	mmol per 1mole steam
1	8	14.01.11	4.64	0.0486
2	27	02.02.11	8.14	0.0522
3	28	03.02.11	9.00	0.0900
5	30	05.02.11	7.92	0.1026
5	31	06.02.11	8.28	0.0882
6	32	07.02.11	9.25	0.0936
7	40	15.02.11	7.31	0.0900
8	51	26.02.11	6.91	0.0288
9	101	17.04.11	10.91	0.0720
10	124	10.05.11	8.14	0.0792
11	131	17.05.11	6.66	0.0828
12	138	24.05.11	8.86	0.1026
13	142	28.05.11	5.94	0.0828
14	156	11.06.11	6.16	0.1656

APPENDIX II : Chemical trends in the discharged fluids of well NWS-6D

Li trend in discharged liquid (NWS-6D)

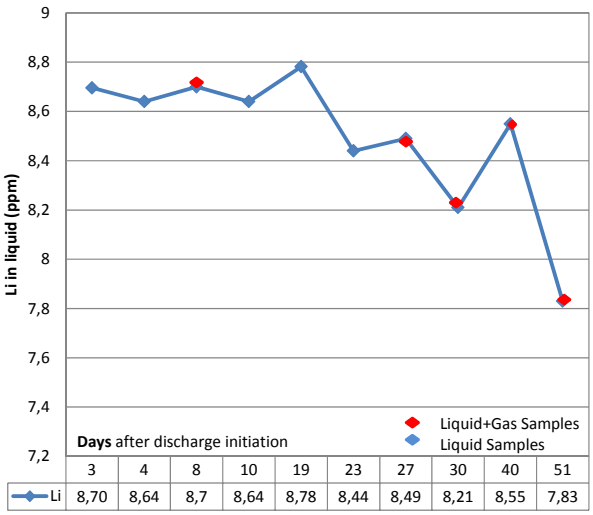

Days after discharge initiation	3	4	8	10	19	23	27	30	40	51
Li	8,70	8,64	8,7	8,64	8,78	8,44	8,49	8,21	8,55	7,83

Na trend in discharged liquid (NWS-6D)

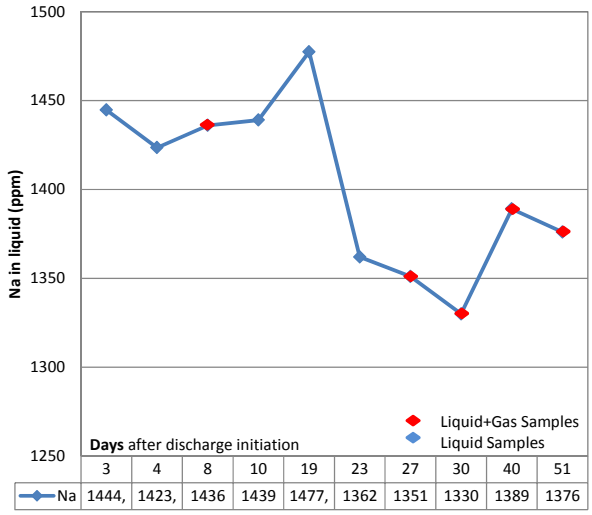

Days after discharge initiation	3	4	8	10	19	23	27	30	40	51
Na	1444,	1423,	1436	1439	1477,	1362	1351	1330	1389	1376

K trend in discharged liquid (NWS-6D)

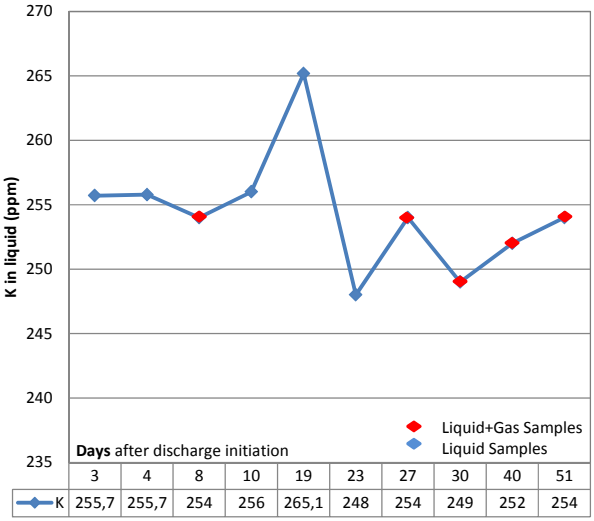

Days after discharge initiation	3	4	8	10	19	23	27	30	40	51
K	255,7	255,7	254	256	265,1	248	254	249	252	254

Ca trend in discharged liquid (NWS-6D)

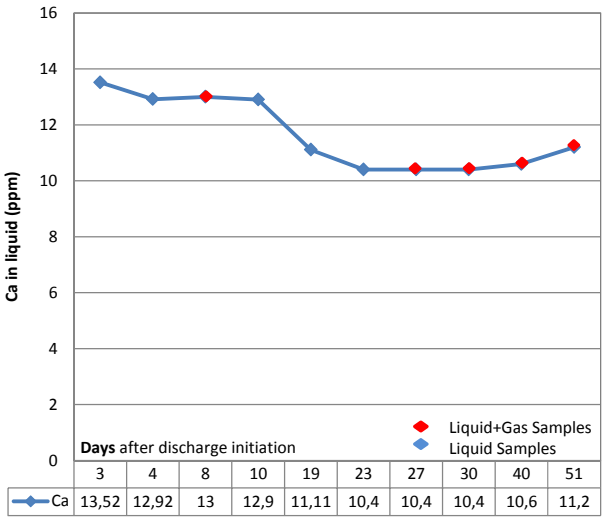

Days after discharge initiation	3	4	8	10	19	23	27	30	40	51
Ca	13,52	12,92	13	12,9	11,11	10,4	10,4	10,4	10,6	11,2

Mg trend in discharged liquid (NWS-6D)

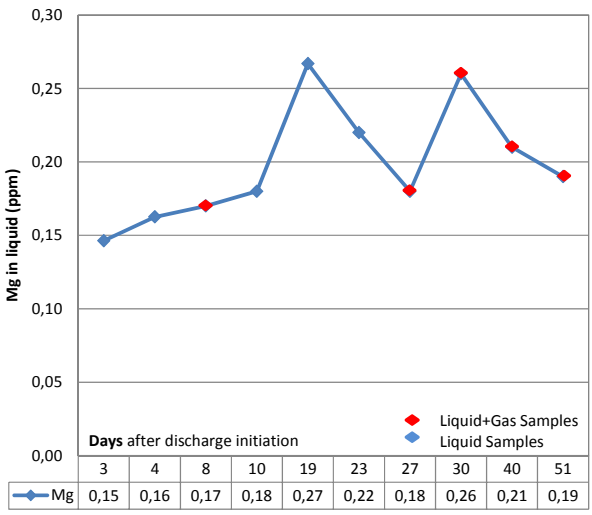

Days after discharge initiation	3	4	8	10	19	23	27	30	40	51
Mg	0,15	0,16	0,17	0,18	0,27	0,22	0,18	0,26	0,21	0,19

Fe trend in discharged liquid (NWS-6D)

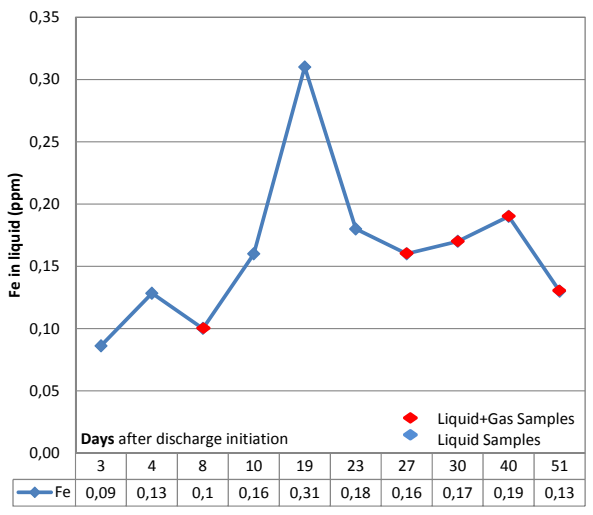

Days after discharge initiation	3	4	8	10	19	23	27	30	40	51
Fe	0,09	0,13	0,1	0,16	0,31	0,18	0,16	0,17	0,19	0,13

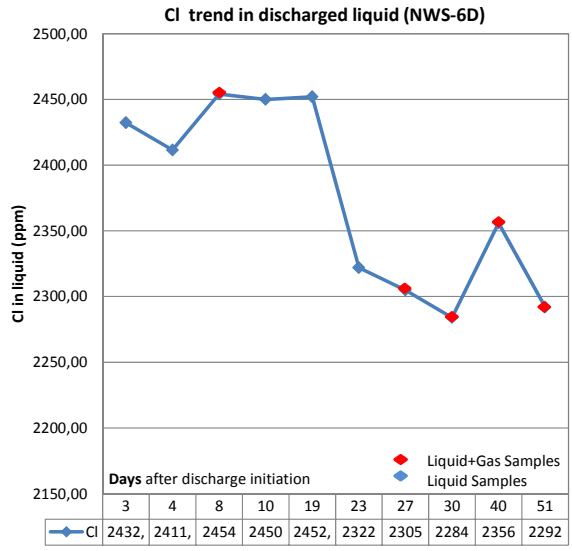

Days after discharge initiation	3	4	8	10	19	23	27	30	40	51
Cl	2432,	2411,	2454	2450	2452,	2322	2305	2284	2356	2292

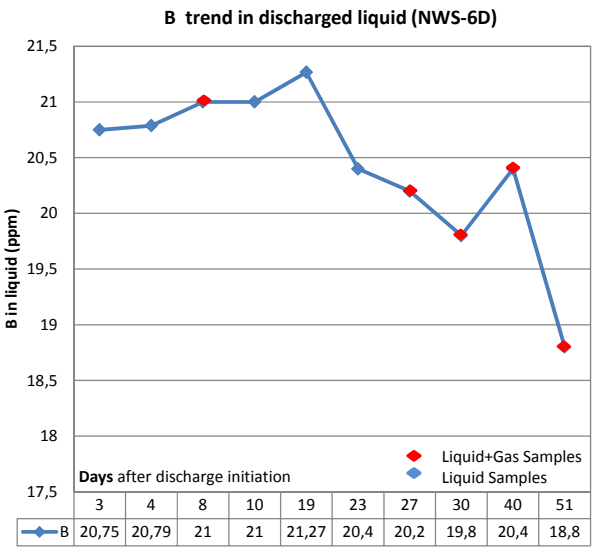

Days after discharge initiation	3	4	8	10	19	23	27	30	40	51
B	20,75	20,79	21	21	21,27	20,4	20,2	19,8	20,4	18,8

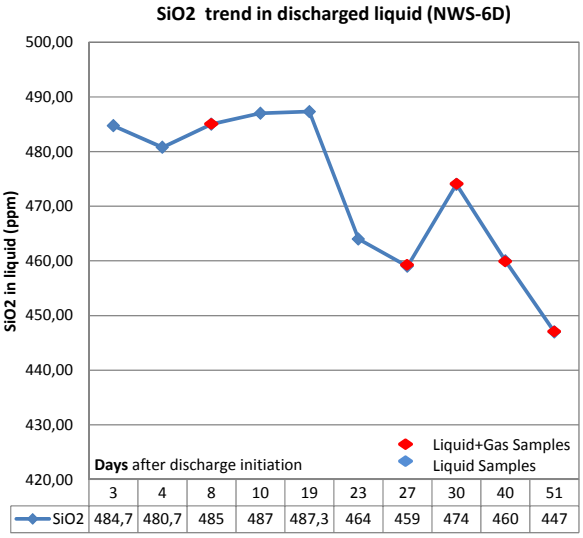

Days after discharge initiation	3	4	8	10	19	23	27	30	40	51
SiO2	484,7	480,7	485	487	487,3	464	459	474	460	447

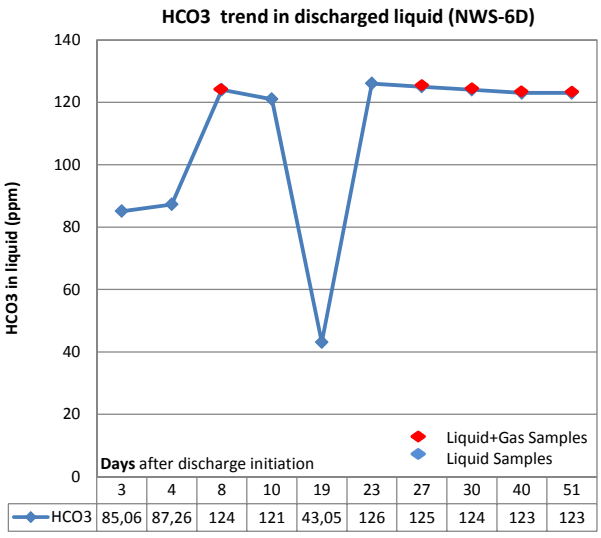

Days after discharge initiation	3	4	8	10	19	23	27	30	40	51
HCO3	85,06	87,26	124	121	43,05	126	125	124	123	123

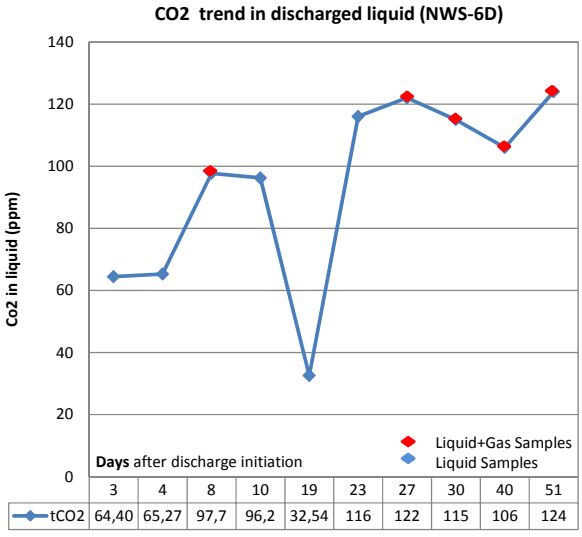

Days after discharge initiation	3	4	8	10	19	23	27	30	40	51
tCO2	64,40	65,27	97,7	96,2	32,54	116	122	115	106	124

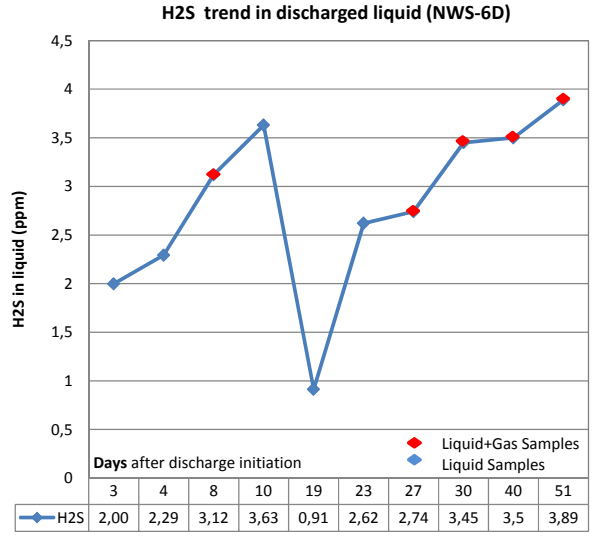

Days after discharge initiation	3	4	8	10	19	23	27	30	40	51
H2S	2,00	2,29	3,12	3,63	0,91	2,62	2,74	3,45	3,5	3,89

SO4 trend in discharged liquid (NWS-6D)

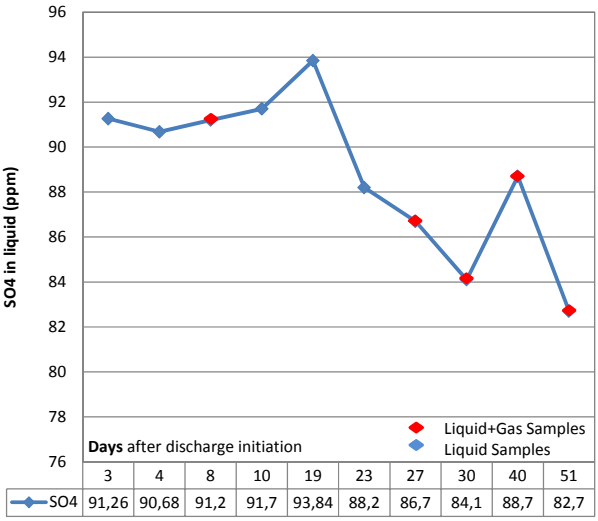

	3	4	8	10	19	23	27	30	40	51
SO4	91,26	90,68	91,2	91,7	93,84	88,2	86,7	84,1	88,7	82,7

NH3 trend in discharged liquid (NWS-6D)

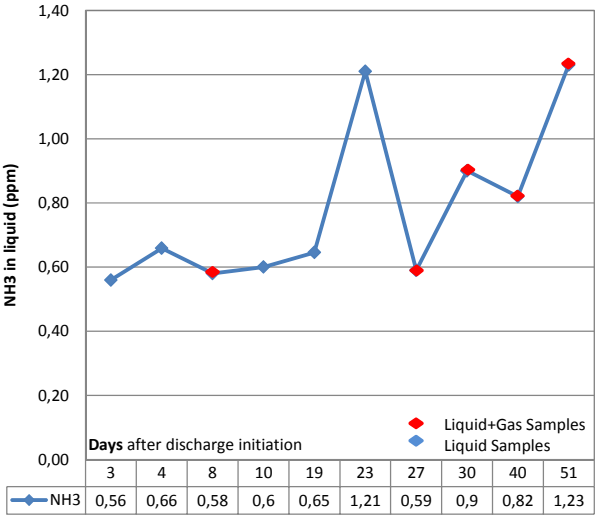

	3	4	8	10	19	23	27	30	40	51
NH3	0,56	0,66	0,58	0,6	0,65	1,21	0,59	0,9	0,82	1,23

F trend in discharged liquid (NWS-6D)

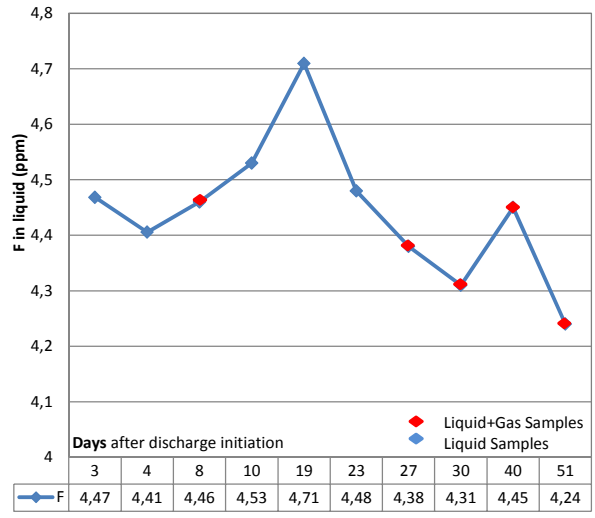

	3	4	8	10	19	23	27	30	40	51
F	4,47	4,41	4,46	4,53	4,71	4,48	4,38	4,31	4,45	4,24

CO2 trend in discharged steam (NWS-6D)

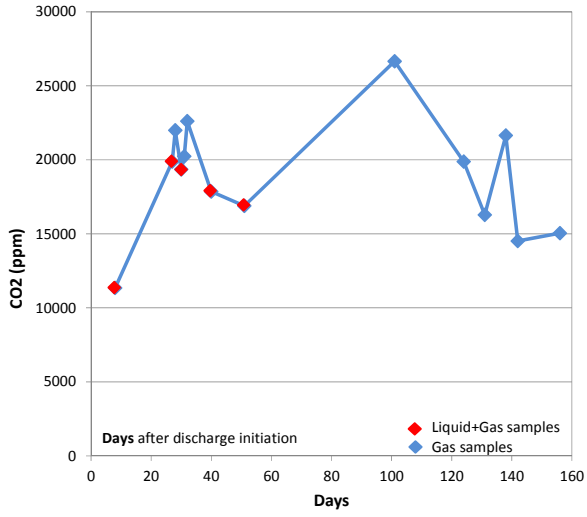

H2S trend in discharged steam (NWS-6D)

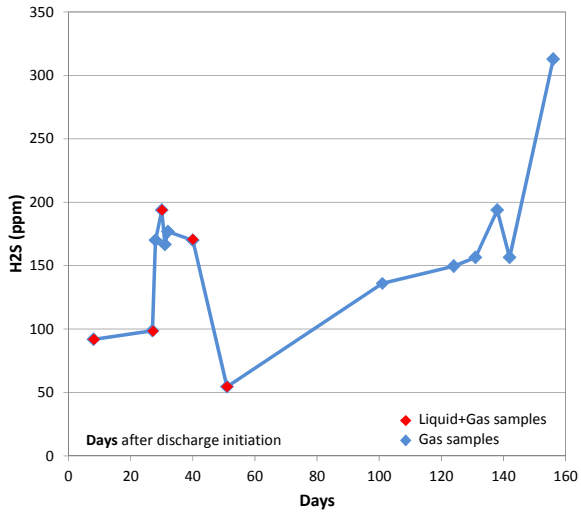

APPENDIX III : Deep fluid chloride concentrations in well NWS-6D correlated with other elements